AFRL-OSR-VA-TR-2015-0123

INNOVATIVE INVERTED MAGNETRON EXPERIMENTS AND THEORY

Ronald Gilgenbach
UNIVERSITY OF MICHIGAN

06/01/2015
Final Report

Air Force Research Laboratory
AF Office Of Scientific Research (AFOSR)/ RTB
Arlington, Virginia 22203
Air Force Materiel Command

REPORT DOCUMENTATION PAGE

Form Approved
OMB No. 0704-0188

PLEASE DO NOT RETURN YOUR FORM TO THE ABOVE ORGANIZATION.

1. REPORT DATE *(DD-MM-YYYY)*	2. REPORT TYPE	3. DATES COVERED *(From - To)*
05-28-2015	Final Report	April 1, 2010 - Feb. 28, 2015

4. TITLE AND SUBTITLE
Innovative Inverted Magnetron Experiments and Theory

5a. CONTRACT NUMBER
FA9550-10-1-0104

5b. GRANT NUMBER
AF0SR-BAA-2009-1

5c. PROGRAM ELEMENT NUMBER

6. AUTHOR(S)
Ronald M. Gilgenbach, Y.Y. Lau, John E. Foster

5d. PROJECT NUMBER

5e. TASK NUMBER

5f. WORK UNIT NUMBER

7. PERFORMING ORGANIZATION NAME(S) AND ADDRESS(ES)
Regents of the University of Michigan
3003 S. State St
Ann Arbor, MI 48109-1274

8. PERFORMING ORGANIZATION REPORT NUMBER

9. SPONSORING/MONITORING AGENCY NAME(S) AND ADDRESS(ES)
Air Force Office of Scientific Research
875 N. Randolph St. Room 3112
Arlington, VA 22203

10. SPONSOR/MONITOR'S ACRONYM(S)
AFOSR

11. SPONSOR/MONITOR'S REPORT NUMBER(S)

12. DISTRIBUTION/AVAILABILITY STATEMENT
Distribution A - Approved for Public Release

13. SUPPLEMENTARY NOTES

14. ABSTRACT
Research at the University of Michigan has designed, simulated, fabricated, and characterized the Recirculating Planar Magnetron (RPM), a new type of High Power Microwave (HPM) device. Researchers have simulated the operation of the device in both a conventional and inverted magnetron geometry, and found the conventional geometry to be more practical. After significant computational iteration, several prototypes were fabricated and tested across a wide parameter space encompassing -250 to -300 kV, 0.18-0.3 T, and pulselengths of 200-500 ns. To improve device operation, multiple cathode designs were simulated and tested, varying both geometry and material properties. The RPM demonstrated peak instantaneous electronic efficiencies as high as 32%, and peak powers of up to 150 MW at 1 GHz. A patent was filed and granted on this RPM device during this grant. A 1.89 GHz variant, the RPM-CACE, has been designed and optimized in collaboration with Air Force Research Lab. Its unique coupler design, the Coaxial All-Cavity Extractor (CACE), provides an efficient, broadband method of power extraction where axial power extraction is desired. In simulation, the RPM-CACE was up to 70% efficient, producing peak microwave powers of 420 MW.

15. SUBJECT TERMS
High power microwaves,

16. SECURITY CLASSIFICATION OF:			17. LIMITATION OF ABSTRACT	18. NUMBER OF PAGES	19a. NAME OF RESPONSIBLE PERSON
a. REPORT	b. ABSTRACT	c. THIS PAGE			Ronald M. Gilgenbach
U	U	U	SAR	36	19b. TELEPHONE NUMBER *(Include area code)* 734 763 1261

Reset

INSTRUCTIONS FOR COMPLETING SF 298

1. REPORT DATE. Full publication date, including day, month, if available. Must cite at least the year and be Year 2000 compliant, e.g. 30-06-1998; xx-06-1998; xx-xx-1998.

2. REPORT TYPE. State the type of report, such as final, technical, interim, memorandum, master's thesis, progress, quarterly, research, special, group study, etc.

3. DATES COVERED. Indicate the time during which the work was performed and the report was written, e.g., Jun 1997 - Jun 1998; 1-10 Jun 1996; May - Nov 1998; Nov 1998.

4. TITLE. Enter title and subtitle with volume number and part number, if applicable. On classified documents, enter the title classification in parentheses.

5a. CONTRACT NUMBER. Enter all contract numbers as they appear in the report, e.g. F33615-86-C-5169.

5b. GRANT NUMBER. Enter all grant numbers as they appear in the report, e.g. AFOSR-82-1234.

5c. PROGRAM ELEMENT NUMBER. Enter all program element numbers as they appear in the report, e.g. 61101A.

5d. PROJECT NUMBER. Enter all project numbers as they appear in the report, e.g. 1F665702D1257; ILIR.

5e. TASK NUMBER. Enter all task numbers as they appear in the report, e.g. 05; RF0330201; T4112.

5f. WORK UNIT NUMBER. Enter all work unit numbers as they appear in the report, e.g. 001; AFAPL30480105.

6. AUTHOR(S). Enter name(s) of person(s) responsible for writing the report, performing the research, or credited with the content of the report. The form of entry is the last name, first name, middle initial, and additional qualifiers separated by commas, e.g. Smith, Richard, J, Jr.

7. PERFORMING ORGANIZATION NAME(S) AND ADDRESS(ES). Self-explanatory.

8. PERFORMING ORGANIZATION REPORT NUMBER. Enter all unique alphanumeric report numbers assigned by the performing organization, e.g. BRL-1234; AFWL-TR-85-4017-Vol-21-PT-2.

9. SPONSORING/MONITORING AGENCY NAME(S) AND ADDRESS(ES). Enter the name and address of the organization(s) financially responsible for and monitoring the work.

10. SPONSOR/MONITOR'S ACRONYM(S). Enter, if available, e.g. BRL, ARDEC, NADC.

11. SPONSOR/MONITOR'S REPORT NUMBER(S). Enter report number as assigned by the sponsoring/ monitoring agency, if available, e.g. BRL-TR-829; -215.

12. DISTRIBUTION/AVAILABILITY STATEMENT. Use agency-mandated availability statements to indicate the public availability or distribution limitations of the report. If additional limitations/ restrictions or special markings are indicated, follow agency authorization procedures, e.g. RD/FRD, PROPIN, ITAR, etc. Include copyright information.

13. SUPPLEMENTARY NOTES. Enter information not included elsewhere such as: prepared in cooperation with; translation of; report supersedes; old edition number, etc.

14. ABSTRACT. A brief (approximately 200 words) factual summary of the most significant information.

15. SUBJECT TERMS. Key words or phrases identifying major concepts in the report.

16. SECURITY CLASSIFICATION. Enter security classification in accordance with security classification regulations, e.g. U, C, S, etc. If this form contains classified information, stamp classification level on the top and bottom of this page.

17. LIMITATION OF ABSTRACT. This block must be completed to assign a distribution limitation to the abstract. Enter UU (Unclassified Unlimited) or SAR (Same as Report). An entry in this block is necessary if the abstract is to be limited.

AFOSR Final Performance Report

Award #: FA9550-10-1-0104

"Innovative Inverted Magnetron Experiments and Theory"

Performance Period: April 1, 2010 – Feb 28, 2015

AFOSR Program Manager:
Jason Marshall
Air Force Office of Scientific Research
875 N. Randolph St. Room 3112
Arlington, VA 22203

Principal Investigator:
Prof. Ronald Gilgenbach
rongilg@umich.edu
(734) 763 – 1261

Co-Principal Investigators
Prof. Y.Y. Lau
yylau@umich.edu
(734) 764-5122
Prof. John E. Foster
jefoster@umich.edu
(734) 764-1976
Nuclear Engineering and Radiological Science Department
University of Michigan
1911 Cooley Building
2355 Bonisteel Blvd.
Ann Arbor, MI 48109

Summary

A novel magnetron concept has been designed, simulated, fabricated, and characterized. Research at the University of Michigan has developed the Recirculating Planar Magnetron (RPM), a new type of High Power Microwave (HPM) device. Using HFSS, MAGIC, and ICEPIC, researchers have simulated the operation of the device in both a conventional and inverted magnetron geometry, and found the conventional geometry to be more practical. After significant computational iteration, several prototypes were fabricated and tested across a wide parameter space encompassing -250 to -300 kV, 0.18-0.3 T, and pulselengths of 200-500 ns. To improve device operation, multiple cathode designs were simulated and tested, varying both geometry and material properties. The RPM demonstrated peak instantaneous electronic efficiencies as high as 32%, and peak powers of up to 150 MW at 1 GHz. A patent was filed and granted on this RPM device during this grant[1]. A 1.89 GHz variant, the RPM-CACE, has been designed and optimized in collaboration with Air Force Research Lab via an iterative design process. Its unique coupler design, the Coaxial All-Cavity Extractor (CACE), provides an efficient, broadband method of power extraction where axial power extraction is desired. In simulation, the RPM-CACE was up to 70% efficient, producing peak microwave powers of 420 MW.

[1] R.M. Gilgenbach, Y.Y. Lau, D. M. French, B. W. Hoff, J. Luginsland, and M.A. Franzi, “Crossed field device," US Patent No.: US8,841,867 B2, Granted September 23, 2014.

Table of Contents

Table of Figures

Introduction

Magnetrons are the "gold standard" for efficient microwave generation, providing robust operation in both military and commercial applications. High power magnetrons have operated for decades in the fields or radar, counter-electronics, communication, and commercial heating. Relativistic (cylindrical) magnetrons, operating in 0.1-1 μs pulses, have demonstrated peak powers of 4 GW and efficiencies of up to 35%.[2,3] When operating in a space-charge limited regime, the available current is constrained by the cathode surface area. Consequently, the total power of the device is limited. For a given impedance, cathode surface area can be increased by increasing the size of the device, but this drives up the weight, total volume, and magnetic field volume (further driving up size, weight, and power requirements). In CW or repetitively pulsed designs, anode heat removal is also a relevant concern.

The Recirculating Planar Magnetron (RPM) is a crossed-field device that combines the advantages of recirculating devices with those of planar devices. The recirculating bends improve device efficiency, while the larger cathode and anode surface areas provide higher current and better heat removal, respectively. Additionally, the magnetic field volume grows only linearly with the number of cavities, N, rather than N^2 for traditional cylindrical designs.

In this work, we have successfully designed, modeled, fabricated, and tested a RPM prototype. Using HFSS, MAGIC, and ICEPIC, we have simulated the operation of the device in both a conventional and inverted magnetron geometry, and have explored several cathode designs, varying both geometry and materials. A unique coupler, the Coaxial All-Cavity Extractor (CACE), has been designed to provide an efficient, broadband method of power extraction where axial power extraction is desired. It has been fielded on the a 1.89 GHz variant, the RPM-CACE, which has been designed and optimized in collaboration with Air Force Research Lab via an iterative design process.

Much of the work described herein was included in a recent University of Michigan Ph.D. dissertation funded by this grant[4].

Methods, Assumptions, and Procedures

Initial Design

Initial RPM development work looked at several embodiments, as shown in Figure 1. While the "racetrack" geometries in A and B offered some distinct advantages (particularly for high frequency designs), the axial B field design in C was chosen for continued development. Initial simulations also investigated the possibility of operating the RPM in an inverted configuration,

[2] T. A. Spencer, "Current HPM Source Research," in High Energy Density and High Power RF (S. H. Gold and G. S. Nusinovich, eds.), vol. 691 of American Institute of Physics Conference Series, pp. 46{46, Dec. 2003.

[3] J. Benford, J. A. Swegle, and E. Schamiloglu, High Power Microwaves, Second Edition. CRC Press, Feb. 2007.

[4] "Relativistic Recirculating Planar Magnetrons" M.A. Franzi, Ph.D. Thesis, University of Michigan, Ann Arbor, 2014.

with the cathode on the outside and the anode in the center, but concerns over microwave power extraction led to the use of a non-inverted design.

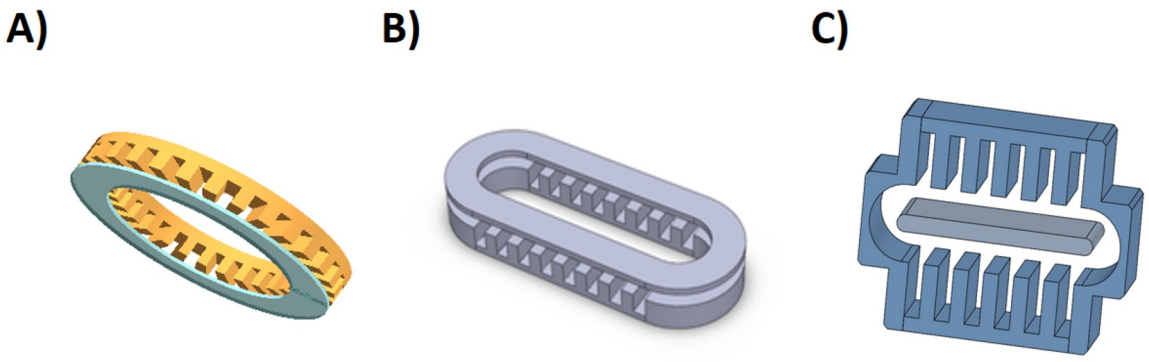

Figure 1: 3D Solidworks renderings of each RPM embodiment including: A) Type (2) with cylindrical cavities, B) Type (2) with planar cavities, and C) Type (1) with planar cavities.

The planar slow-wave structure utilizes π-periodic rectangular cavities to support the desired operating mode. Device dimensions were chosen to fit within existing hardware and develop π-mode oscillations at 1 GHz. The smoothbore cylindrical sections on the ends are designed to recirculate the beam, and provide minimal coupling between the top and bottom oscillators. More complex recirculating section geometries were investigated in simulation to provide more efficient beam recirculation, but were ultimately excluded from the prototype to reduce the complexity of the device.

Throughout the development process, we conducted simulations of this geometry using a 3-D PIC code, MAGIC[5]. Initial simulations and experiments used a 2 cm AK gap and a 5 cm thick hollow cathode, as shown in Figure 2. The anode cavities and vanes had a depth of 6.31 cm, a width of 1.92 cm, and an axial length of 11 cm, leading to a phase velocity of 0.26*c*. The radius of the cylindrical bends was set at 4.5 cm to maintain a beam velocity of 0.25-0.3*c* over the expected operating parameters. Later designs reduced the cathode thickness to increase the AK gap and reduce the effects of diode gap closure.

RPM-12a

After substantial iteration, we settled on a 12-cavity design with a 3.9 cm AK gap spacing and a solid, 1.27 cm thick, 24 cm long, 17 cm deep cathode, known as the LC-1. This RPM prototype is known as the RPM-12a. Figure 3 illustrates this geometry, as well the spoke formation when the device is simulated in MAGIC. The Michigan Electron Long Beam Accelerator with Ceramic stack (MELBA-C) was the pulsed power driver for the RPM prototype, and was capable of providing cathode voltages of -250-300 kV, 0.15-0.32 T axial magnetic fields, and 500 ns pulse durations. These parameters also influenced the design of the initial prototype.

In many instances, we show the RPM in a horizontal configuration, or refer to the anode structures as “top” and “bottom”. In practice, the device is actually operated with the cathode

[5] http://www.mrcwdc.com/Magic/description.html

running vertically, due to the long moment arm of our cathode stalk. A slight cathode droop in the horizontal configuration leads to a smaller AK gap on the bottom, preferential current emission from that side, and increased change of gap closer on that side. In the vertical configuration, if the cathode sags slightly then it is closer to one of the recirculating bends, which has less of an impact on operation. One consequence of this orientation, however, is that any arcing from the end hats to the recirculating bends is likely to be on the bottom of the device.

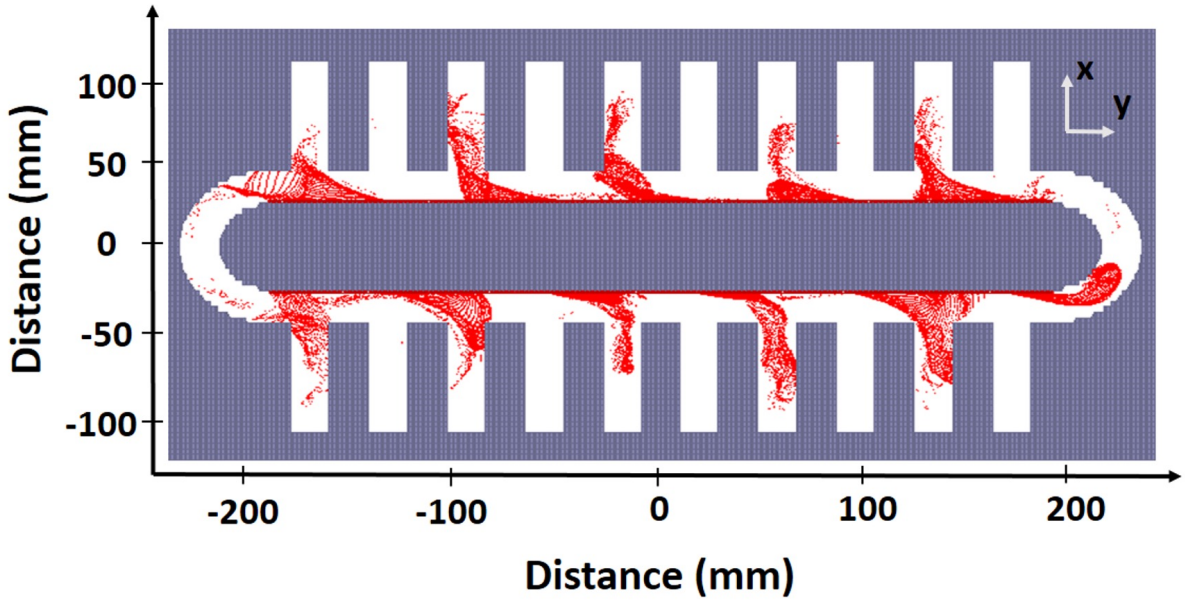

Figure 2: 2D simulation in MAGIC PIC of the initial L-band RPM prototype. The magnetic field points out of the paper.

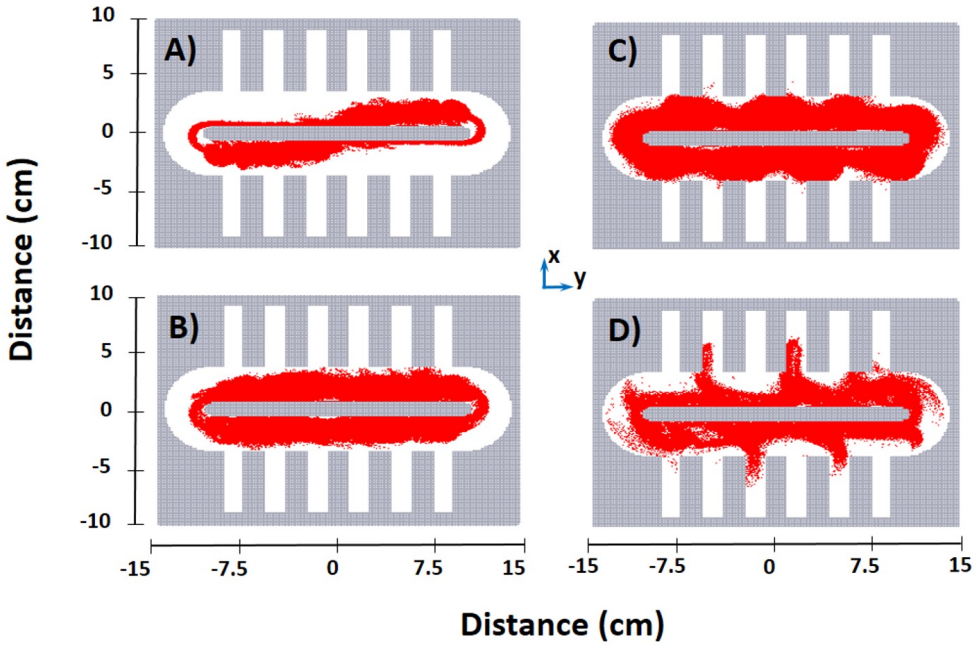

Figure 3: Simulated magnetron operation (in MAGIC PIC) of the RPM-12a with solid cathode for varying stages of mode development including: A) Initial electron emission (19 ns), B) Brillouin flow and electron hub formation (24 ns), C) RF perturbations on laminar flow (43 ns), and D) Full pi-mode operation (60 ns).

The finite element program, Ansoft's High Frequency Structure Simulator (HFSS), was also used extensively in the design of the RPM to validate MAGIC cold tests and identify modes of operation. As shown in Figure 4, the initial RPM prototype had closely spaced even and odd π-modes, leading to mode competition and beating between each oscillator. The smoothbore recirculating sections do not keep the beam fully bunched, leading to weakly coupled top and bottom oscillators.

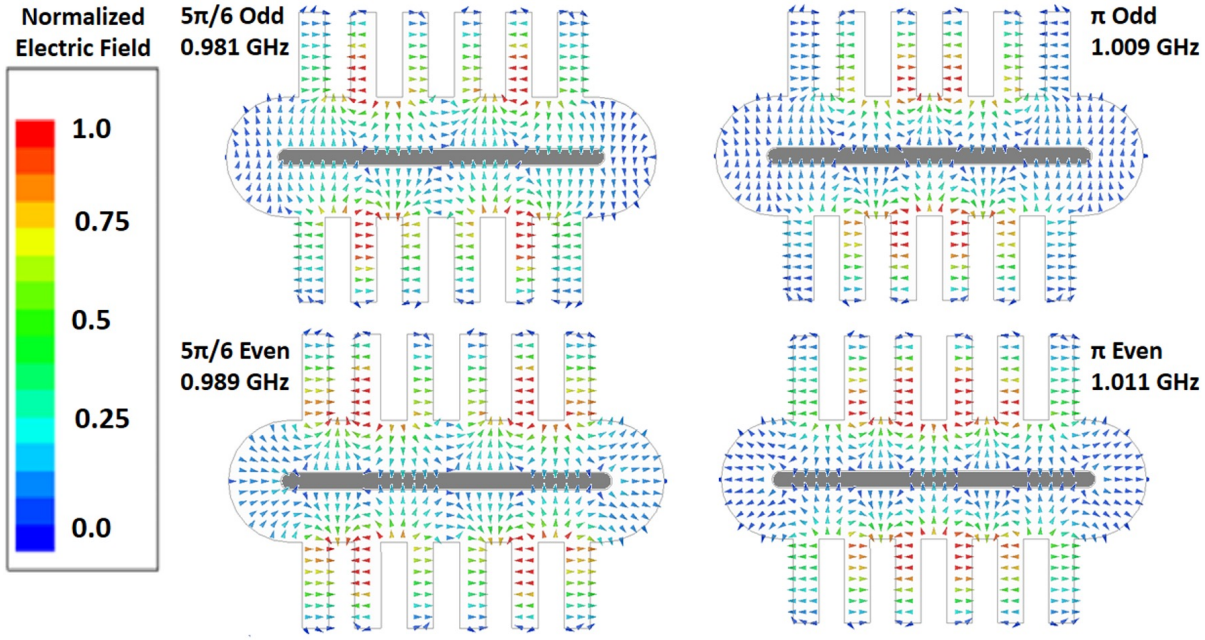

Figure 4: Electric field configurations for the even and odd 5pi/6 -modes (left) and pi-modes (right) found using HFSS.

MCC-1

To address this issue, we designed and implemented a Mode Control Cathode (MCC), which acts as a resonant electromagnetic coupler, as well as an emission priming structure, similar to the transparent cathode.[6] Fundamentally, the MCC is an array of conductors that matches the vane-cavity periodicity of the RPM. The MCC increases the separation between the even and odd π-modes by altering the boundary condition along its horizontal axis of symmetry, where the differences between the even/odd modes are most pronounced (Figure 5).

[6] M.I. Fuks and E. Schamiloglu, "Rapid Start of Oscillations in a Magnetron with a "Transparent Cathode"," Phys. Rev. Lett., vol. 95, 205101-1-4 (2005)

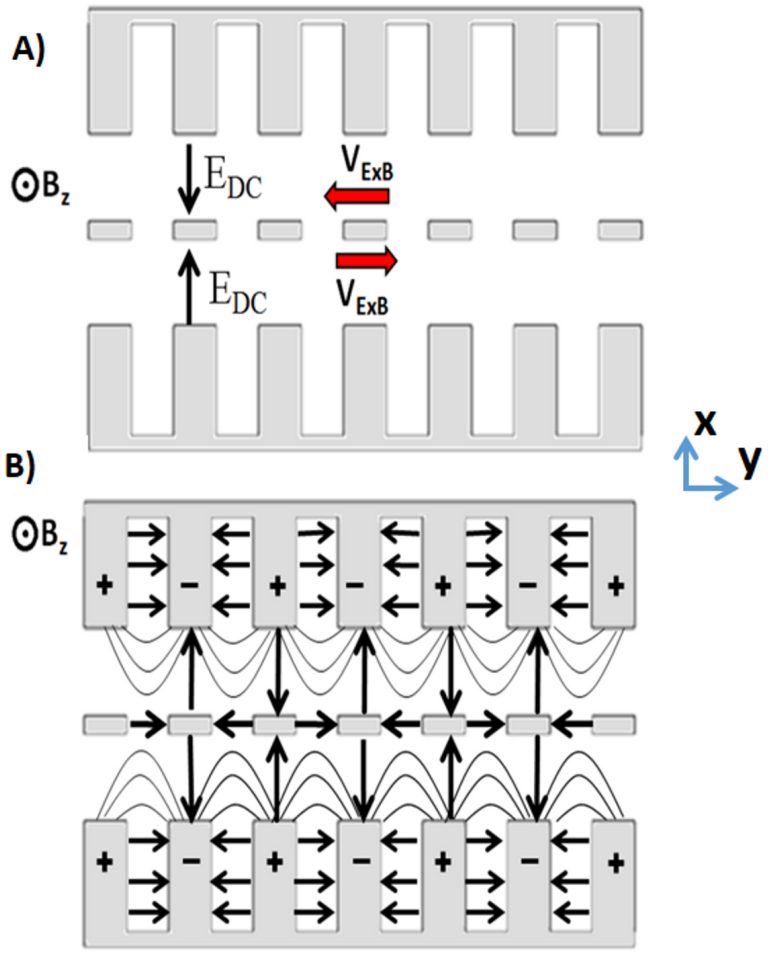

Figure 5: 2D representation of the Mode Control Cathode geometry in the RPM with: A) DC electric and magnetic fields as well as beam drift direction (shown in red), and B) RF electric field configuration.

Analytic Theory Development

As part of this work, we developed an analytical solution for the dispersion relation of the MCC[7], and will summarize it here.

The dispersion relation for the MCC geometry is solved using the classic approach for an infinite cavity array.[8] We represent the geometry with a single vane-cavity structure, shown in Figure 6, and apply the Floquet Theorem to replicate this structure as an infinite array. To obtain the resonant frequency, we decompose the structure into 3 distinct vacuum regions: 1) AK gap: vacuum region between cathode and anode, 2) Cathode space: vacuum region within the interior of the cathode, and 3) Resonant Cavity: vacuum region within the interior of the anode.

[7] M. Franzi, R. Gilgenbach, Y. Y. Lau, B. Hoff, G. Greening, and P. Zhang, "Passive mode control in the recirculating planar magnetron," Physics of Plasmas, vol. 20, p. 033108, Mar. 2013.
[8] Y. Y. Lau and D. Chernin, "A review of the ac space charge effect in electron circuit interactions," Physics of Fluids: Plasma Physics, vol. 4, pp. 3473-3497, Nov. 1992.

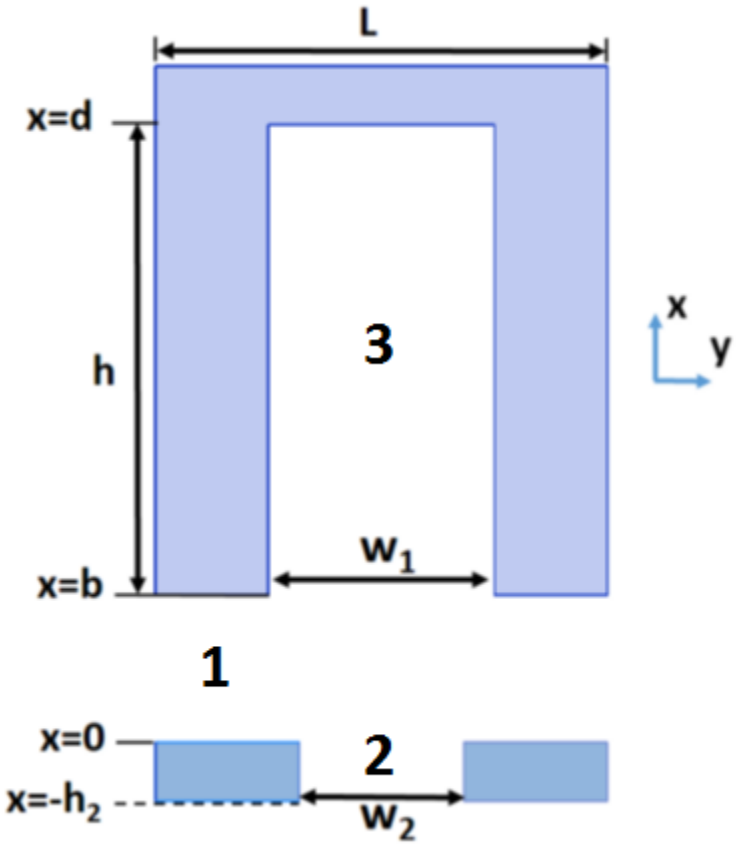

Figure 6: Single period of the RPM slow wave structure with MCC showing the three regions of vacuum: I) the AK gap, II) the gap in the cathode, and III) the resonant cavity. The horizontal axis, *x* = -h_2, bisects the RPM into two halves.

We then solve the EM fields of each region and use the solutions to match the RF fields along the 2 boundaries (1/2 at x=0 and 1/3 at x=b). It is assumed that the modes in regions 2 and 3 are TEM modes, as they the only important components for magnetron operation.

The two-fold symmetry of the RPM requires a unique boundary condition along the center line at x = -h_2. If this is categorized as a perfect E_y (null) boundary, there will be a 180° phase shift in E_y across the boundary and the odd mode solution will result. Similarly, a perfect H_z (null) boundary produces the even mode solution with a 0° phase shift in E_y across the boundary. The resulting dispersion relation for the even modes:

$$UV = -YZ \qquad \text{Eqn 1}$$

$$V = \sin\left(\frac{\omega h_2}{c}\right) + \cos\left(\frac{\omega h_2}{c}\right) \sum_{n=-\infty}^{\infty} \frac{\omega}{\gamma_n c} \frac{w_2}{L} sinc^2(\theta_2) coth(\gamma_n b) \qquad \text{Eqn 2}$$

$$U = \cos\left(\frac{\omega h}{c}\right) - sin\left(\frac{\omega h}{c}\right) \sum_{n=-\infty}^{\infty} \frac{\omega}{\gamma_n c} \frac{w_1}{L} sinc^2(\theta_1) coth(\gamma_n b) \qquad \text{Eqn 3}$$

$$Z = \frac{w_1}{L} \sum_{n=-\infty}^{\infty} \frac{\omega}{\gamma_n c} \frac{sin\left(\frac{\omega h}{c}\right)}{\sinh(\gamma_n b)} sinc(\theta_2) sinc(\theta_1) \qquad \text{Eqn 4}$$

$$Y = \frac{w_2}{L}\sum_{n=-\infty}^{\infty}\frac{\omega}{\gamma_n c}\frac{cos\left(\frac{\omega h_2}{c}\right)}{\sinh(\gamma_n b)}sinc(\theta_2)sinc(\theta_1) \qquad \text{Eqn 5}$$

Similarly, the odd-mode dispersion relation is:

$$U`V` = -Y`Z` \qquad \text{Eqn 6}$$

$$V` = \cos\left(\frac{\omega h_2}{c}\right) - \sin\left(\frac{\omega h_2}{c}\right)\sum_{n=-\infty}^{\infty}\frac{\omega}{\gamma_n c}\frac{w_2}{L}sinc^2(\theta_2)coth(\gamma_n b) \qquad \text{Eqn 7}$$

$$U` = \cos\left(\frac{\omega h}{c}\right) - sin\left(\frac{\omega h}{c}\right)\sum_{n=-\infty}^{\infty}\frac{\omega}{\gamma_n c}\frac{w_1}{L}sinc^2(\theta_1)coth(\gamma_n b) \qquad \text{Eqn 8}$$

$$Z` = \frac{w_1}{L}\sum_{n=-\infty}^{\infty}\frac{\omega}{\gamma_n c}\frac{sin\left(\frac{\omega h}{c}\right)}{\sinh(\gamma_n b)}sinc(\theta_2)sinc(\theta_1) \qquad \text{Eqn 9}$$

$$Y` = \frac{w_2}{L}\sum_{n=-\infty}^{\infty}\frac{\omega}{\gamma_n c}\frac{cos\left(\frac{\omega h_2}{c}\right)}{\sinh(\gamma_n b)}sinc(\theta_2)sinc(\theta_1) \qquad \text{Eqn 10}$$

When w_2 approaches zero, the system reduces to a solid cathode with a perfectly conductive boundary at x=0. Correspondingly, Y and U will go to zero. With U=0, Eqn 3 yields the known planar cavity array expression:

$$\cos\left(\frac{\omega h}{c}\right) = \sum_{n=-\infty}^{\infty}\frac{\omega}{\gamma_n c}\frac{w_1}{L}sinc^2(\theta_1)coth(\gamma_n b) \qquad \text{Eqn 11}$$

Simulation

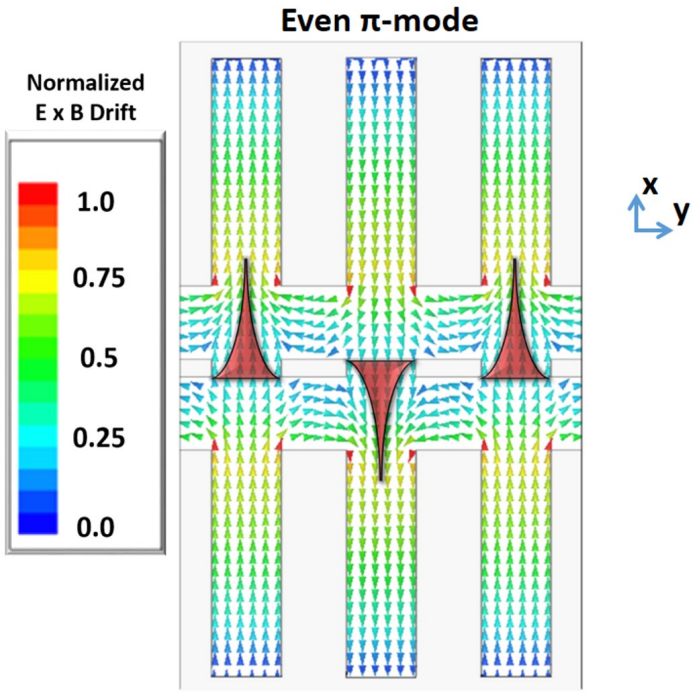

Figure 7: Sample section of the RPM slow wave structure and MCC with arrows representing the normalized magnitude and direction of the E_{RF} x B drift experienced by the particles as well as the spoke formation caused by these drifts (shaded red).

The electron self-focusing effect in each top/bottom cavity pair, was anticipated to greatly improve the coupling between the top and bottom oscillators, generate faster startup, and improve mode stability. The even/odd π-modes with a solid cathode were separated by only 2 MHz, as shown in Figure 4. The analytic and numerical dispersion relations for the MCC shown in Figure 8, however, demonstrate that it improves the mode separation to over 40 MHz. This separation continues to improve as the AK gap approaches zero, and asymptotically approaches zero as the AK gap is increased beyond 3 cm. Practical constraints of gap closure limit the AK gap to a minimum of 2 cm. Figure 8 also demonstrates excellent agreement between the analytic theory and simulation results for an infinite cavity array.

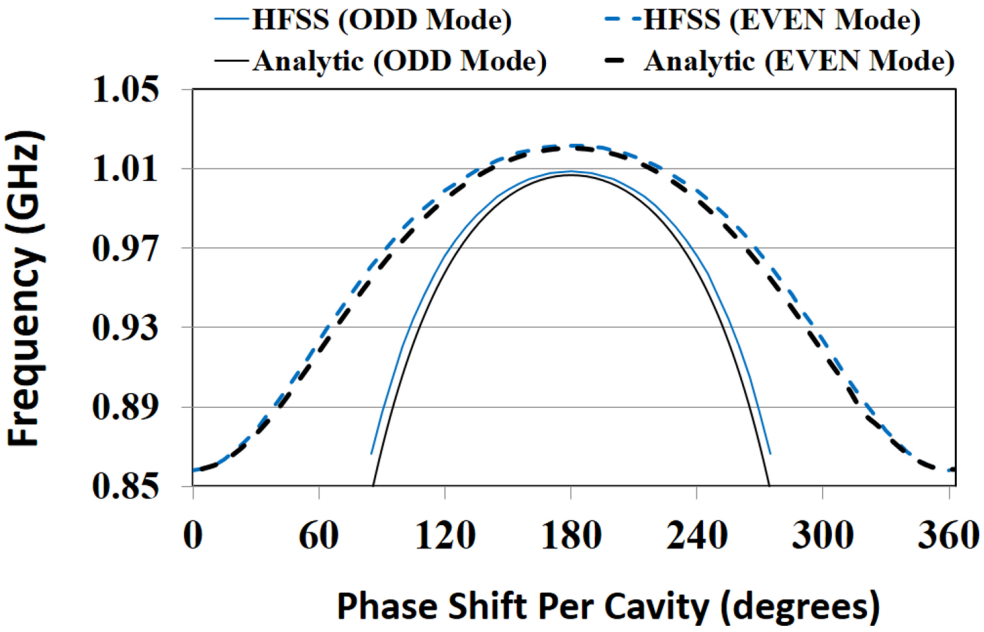

Figure 8: Dispersion relation including the mode control cathode for the even (Dashed-black) and odd (black) modes using the analytic model compared to the even (dashed-blue) and odd (blue) modes in the infinite cavity array in HFSS.

The first mode control cathode design, the MCC-1, was composed of 5 aluminum cylinders, each with a 2.22 cm diameter, spaced 3.8 cm apart, forming an AK gap of 3.38 cm. Each rod was press-fit into two 30 cm long, 5.1 cm diameter end caps spaced 17 cm apart. After issues with arcing from the end hats to the recirculating bends, the end hats separation was increased to 22 cm, as shown in Figure 9, and the cathode was denoted as the MCC-1L. A subsequent variant, the MCC-1Lg, was Glyptal coated to suppress emission outside of the interaction region.

Figure 9: The MCC-1 cathode, mounted on the cathode stalk with the anode and vacuum chamber removed. It consists of five, 2.2 cm OD rods spaced 3.8 apart, resulting in an AK gap of 3.34 cm.

While the MCC-1 did produce the desired phase-locking and mode purity, it was not highly reproducible. The large AK gap limited the cross-oscillator coupling, as the magnitude of the RF field on the cathode surface falls off with increased anode-cathode separation. The benefits of the MCC-1 were incorporated into its successor, which attempted to address its shortcomings.

MCC-2

The MCC-2, designed to reduce the effective AK gap of the RPM diode, was composed of 5 hollow, 1.9×3.8 cm rectangular structures, resulting in an AK gap of 2.6 cm; including the end caps, it was 23 cm in length (Figure 10). To suppress undesirable emission, the end caps of both MCCs were coated with Glyptal insulating paint. The final embodiment of the MCC-2 added 1.9 cm^2 velvet squares to the center of the cathode using conductive silver epoxy adhesive (Figure 11d).

Figure 10: MCC-2 cathode with Glyptal paint coating. The emission regions in the center are left bare and given a high surface roughness to enhance emission.

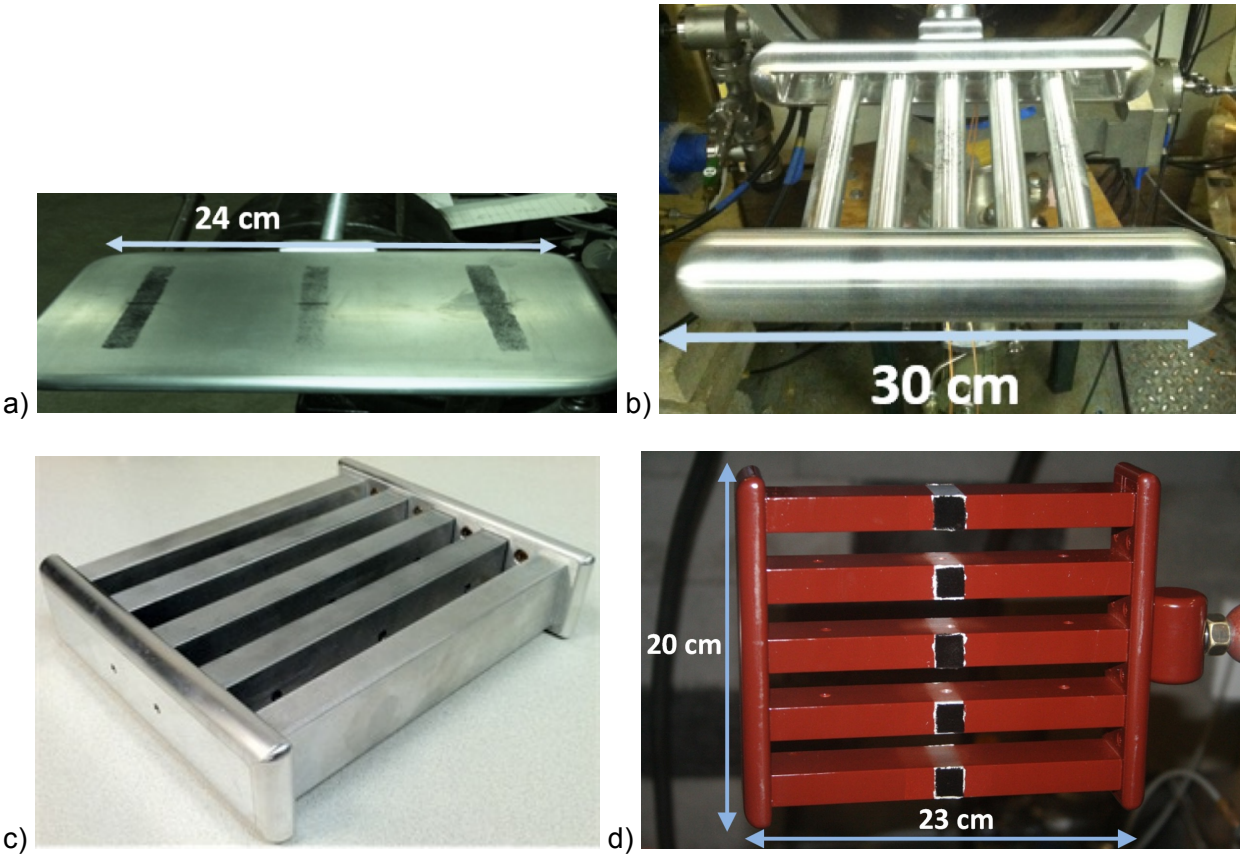

Figure 11: A comparison of all cathodes tested in the RPM-12a. a) LC-1 b) MCC-1 c) MCC-2 d) MCC-2 with Glyptal paint and velvet emitters.

Power Extraction Design

Power extraction for the RPM was a two-stage process, consisting of the Proof-of-Principle (PoP) coaxial extractor, and the Coaxial All Cavity Extractor (CACE). Extractor designs were largely constrained by the existing experimental setup and available space. Coaxial extraction was determined to be most promising, but additional hardware was required to convert the coaxial transmission line to an easily measured TE_{10} waveguide mode. This was accomplished using a distributed field adapter (DFA). The DFA is designed to minimize electric field enhancement on its surface by distributing the axial Poynting flux over a broad, smooth, conductive surface. Elongating the conductive structures distributes the power and extends the transitional TE_{11} mode in the axial direction. Two DFAs were manufactured for this experiment. The first, shown in Figure 12a, was used in the PoP coupler in WR-650 waveguide. The second, Figure 12c, was the basis for the RPM-CACE coupler in WR-340 waveguide.

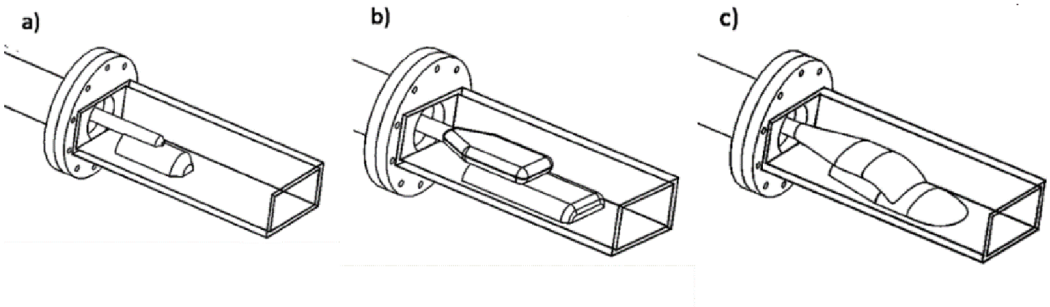

Figure 12: a) Cylindrical cross-section DFA, the simplest design. b) A rounded rectangular cross-section DFA. c) The elliptical cross section DFA.

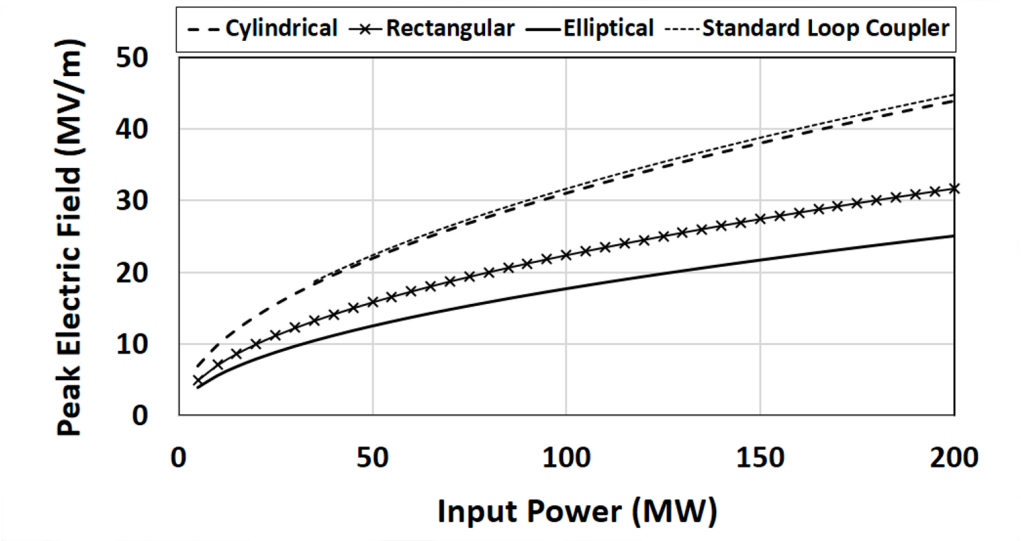

Figure 13: Peak electric field of each coupler design as a function of input power. The elliptical design, while complex to manufacture, demonstrates excellent performance.

PoP Coupler (DFA-650b)

The PoP coupler was designed to have a pass band at 0.93-1.08 GHz, exceeding the expected operating range of the RPM-12a and interfacing with the WR-650 waveguide components already in place. A dimensional schematic of this DFA is shown in Figure 12. Parameters A through E were set by the readily available materials sizes. Given these constraints and the pass-band target, the remaining parameters (F-H) were optimized through numerical iteration in an HFSS script. For simulated input powers of 100 MW, the peak fields in the coupler were 32 MV/m (Figure 13).

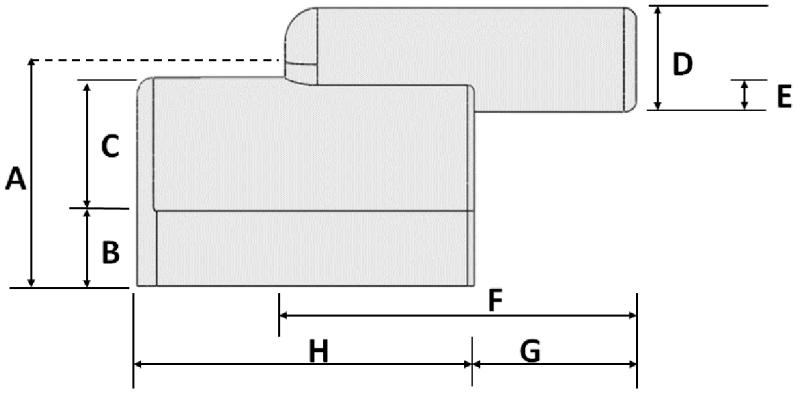

Figure 14: Longitudinal cross section of the PoP DFA, indicating the dimensions used for design and fabrication. A= 8.3 cm, B= 1.27 cm, C= 2.54 cm, D= 1.9 cm, E= 0.32 cm, F= 6.1 cm, G= 2.8 cm, H= 6.6 cm

DFA-340e

The DFA-340e, designed for use on the RPM-CACE at 1.9 GHz, expanded on the PoP coupler to provide greater power handling and improved bandwidth. Its elliptical profile, shown in Figure 15, was highly optimized via extensive HFSS simulation. While some iterations of the DFA-340 demonstrated bandwidths in excess of 35%, the final 'e' design was relatively narrow band, sacrificing bandwidth for improved transmission over the intended 1.85-1.95 GHz operating range, as shown in Figure 16.

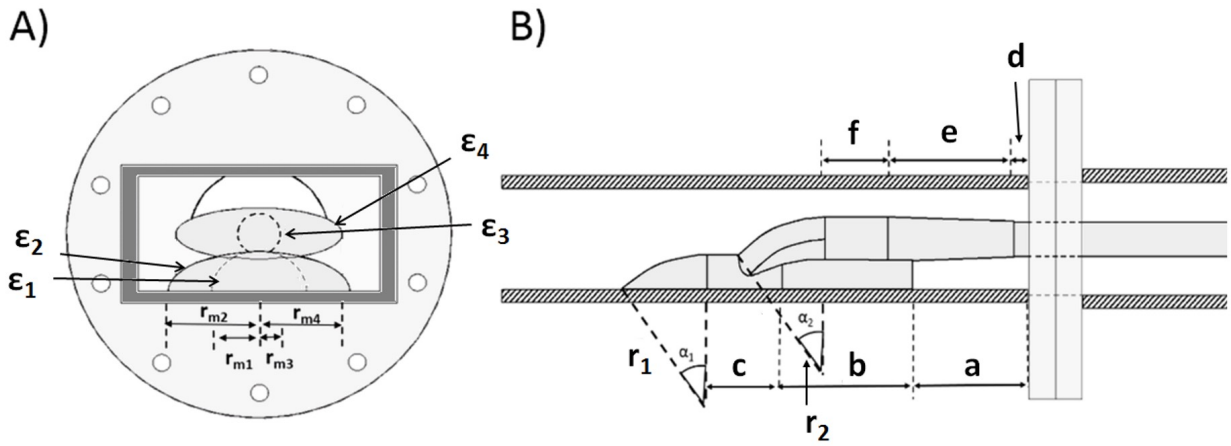

Figure 15: A) Transverse cross section of the elliptical DFA with relevant dimensions, and B) Longitudinal cross section of the elliptical DFA with relevant dimensions shown in Table 1.

Table 1: Optimized dimensions of the DFA-340e for transmission and minimal electric field enhancement from 1.85 to 2 GHz.

Parameter	Value (cm)	Parameter	Value
a	6.6	ε_1	0.33
b	6.2	ε_2	0.47
c	3.5	ε_3	1.00
d	1.36	ε_4	0.325
e	6.0	rm_1	1.7 cm
f	3.0	rm_2	3.2 cm
r_1	5.0	rm_3	0.75 cm
r_2	5.0	rm_4	3.0 cm

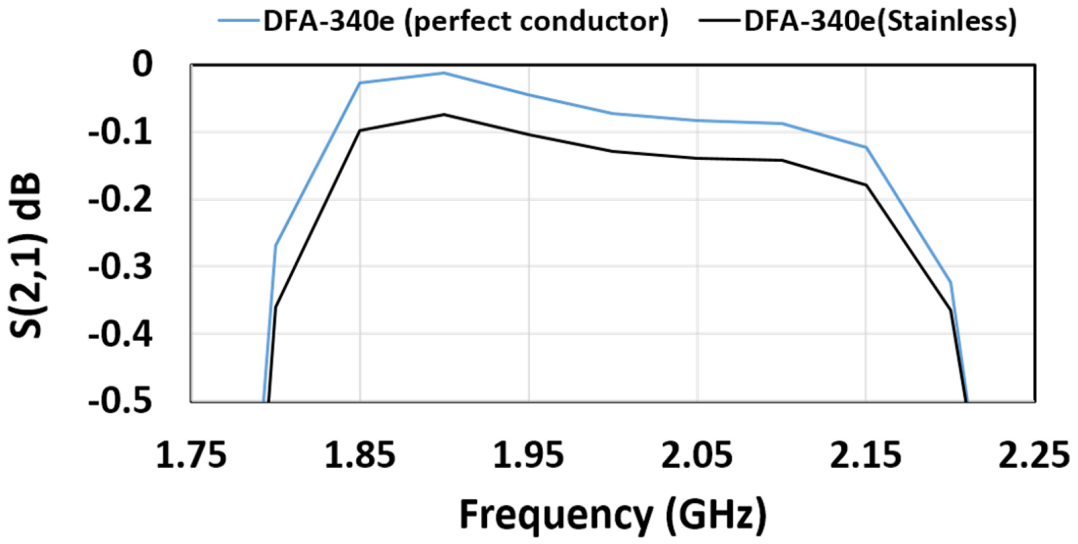

Figure 16: Transmission properties of the DFA-340e for both a perfect conductor (blue), and the actual fabrication material (black).

Experimental Setups

The Michigan Electron Long Beam Accelerator with a Ceramic insulator stack (MELBA-C) was used to operate the RPM-12a at voltages between -250 and -300 kV for pulselengths of 200–600 ns. Pulsed electromagnets were placed approximately 21.6 cm apart in a pseudo-Helmholtz configuration and centered over the anode region to create a nearly uniform axial magnetic field, which was varied on a per-shot basis from 0.1–0.34 T. The magnetron was housed within a cylindrical, 63.5 cm long, 39.4 cm diameter, #304 stainless steel vacuum chamber and was operated at vacuums between 10^{-6}-10^{-7} Torr. The MELBA-C voltage pulse was sampled by a $CuSO_4$ resistive divider and the current entering the RPM-12a was measured by a Rogowski coil embedded in the MELBA-C output port.

Phase Measurements

In the initial RPM-12a experiments, a calibrated power extraction scheme had not yet be implemented, and the experiments focused on phase measurements via 2 mm^2 B-dot probes placed ~4 mm axially from the central open-ended cavity of the two slow wave structures (Figure 17). Signals from each B-dot loop were transmitted via identical N-type cables to 4 GHz, 20 GS/s Tek7404 oscilloscopes in a Faraday cage for measurement.

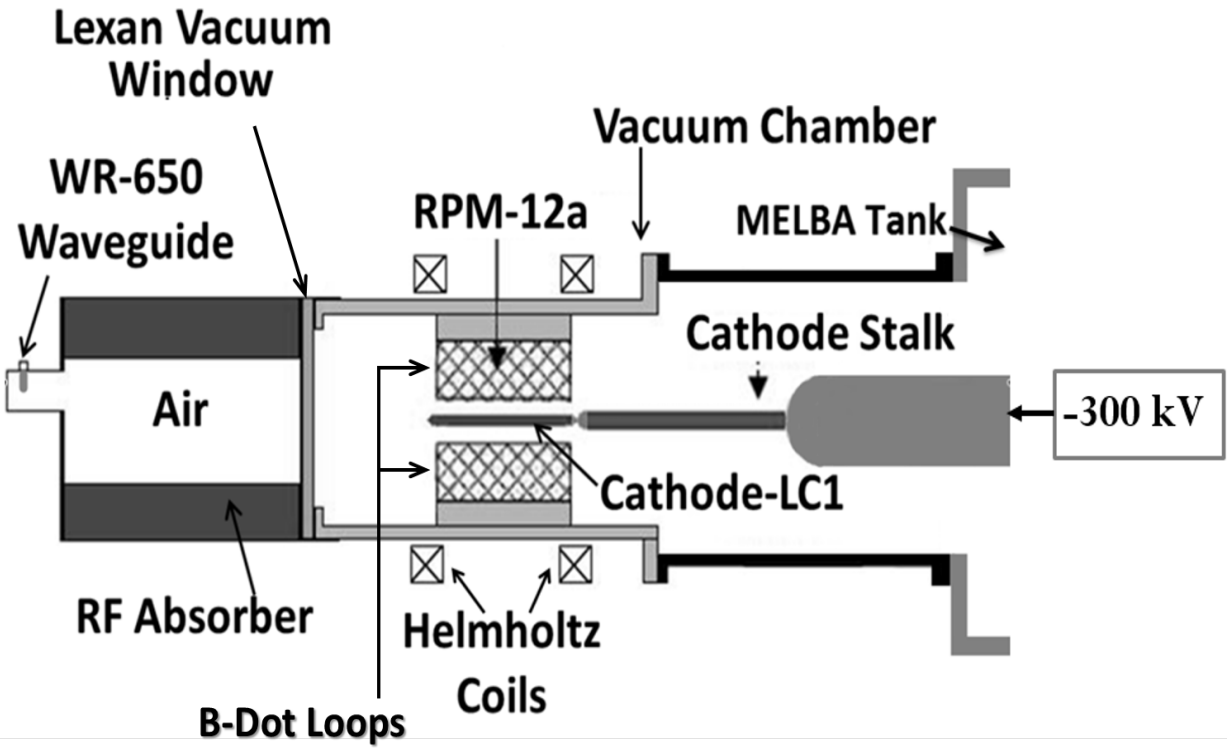

Figure 17: Cross-sectional top view of the experimental setup for initial phase measurements of the RPM-12a with LC1 and MCC-1 cathodes. Power is diffraction coupled out of the end of magnetron and sampled by an uncalibrated loop coupler. Oscillations on each slow wave structure are monitored with B-dot loops.

Calibrated Power Measurements

Subsequent experiments to make calibrated power measurements replaced the Lexan vacuum window with a 1" thick aluminum flange, to which the couplers and outer coaxial conductors are mounted (Figure 18). A 1.5 cm OD aluminum rod connects to the center vane of each anode, as well as to the input of the DFA-650b. Directional couplers (-58 dB), are mounted to the output of each coupler, and terminate in Ecosorb loads (Figure 19). The output of the couplers is transmitted to a Faraday cage and attenuated with 20-25 dB of additional inline attenuation, then split with a two-way power divider to be directly sampled by the Tek7404 oscilloscope and rectified by calibrated Agilent 8427B low-barrier Schottky diodes, which are then sampled by 500 MHz, 1 GS/s Tek3054 oscilloscopes.

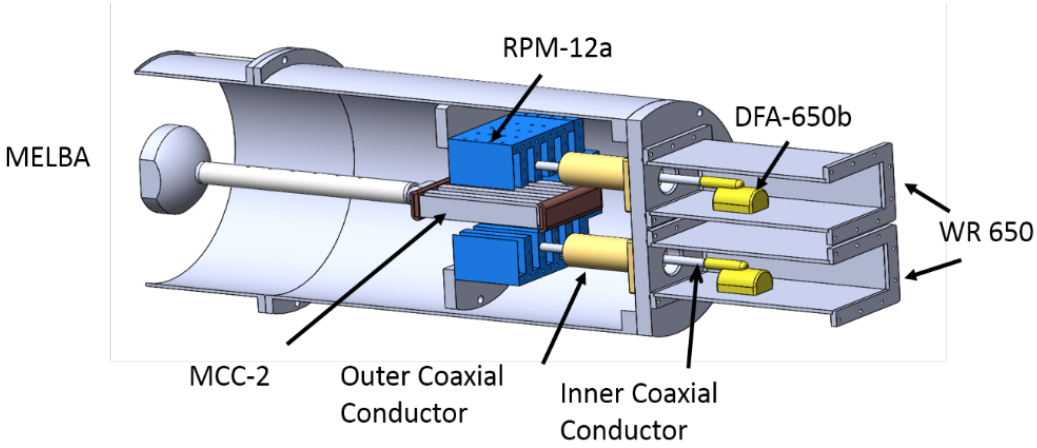

Figure 18: Cut-away top view of the experimental setup for calibrated power measurements. The proof of principle DFA-650b couplers launch a TE_{10} mode into the waveguide, where microwaves can be sampled by directional couplers and then terminated in an Ecosorb load.

Figure 19: Photograph of the experimental setup with the DFA-650b couplers, directional couplers, and Ecosorb loads installed on the end of the magnetron chamber.

RPM-CACE

While the coaxial design of the proof of principle experiment was a success, we wanted to design a more robust power extraction system. With the assistance of Air Force Research Lab, we were able to design and fabricate a 1.9 GHz RPM with a Coaxial All Cavity Extraction (CACE) system. The CACE is derived from the all cavity extractor concept developed by Dr. Greenwood at AFRL[9]. Originally designed for a double baffled waveguide on the A6 magnetron, it uses a slotted waveguide antenna excited by the orthogonal radiation pattern produced by the magnetron.

[9] A. D. Greenwood "All cavity magnetron axial extractor", U.S. Patent 7 106 004, 2006.

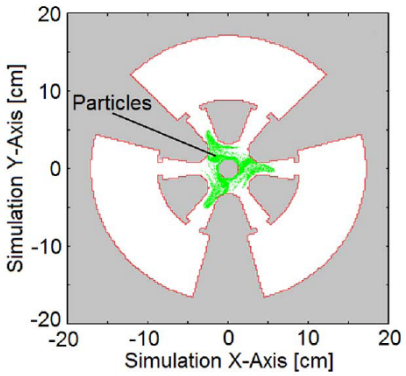

Figure 20: A PIC simulation of the A6 magnetron with axial all cavity extraction, showing the geometry of the concept. [10]

The natural extension of this concept to the planar geometry of the RPM is to "unfold" it to produce a structure similar to what is shown in Figure 21.

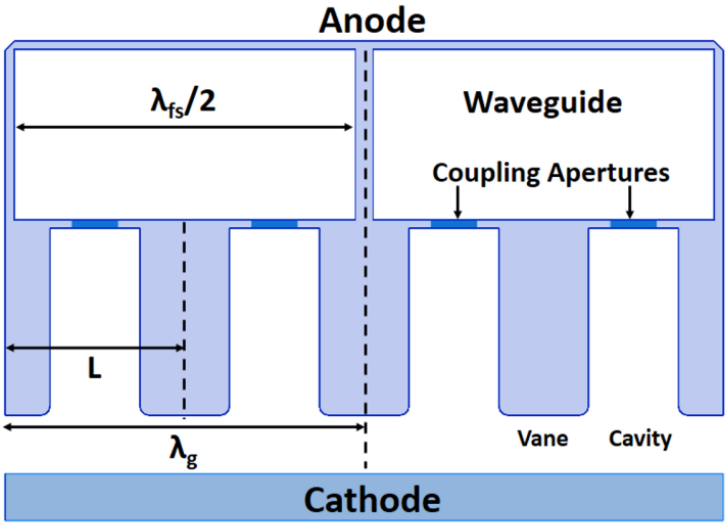

Figure 21: A 2D cross-section of an all-cavity extraction anode using standard rectangular waveguide on a planar RPM geometry.

In this configuration, however, the guided wavelength for π-mode operation is equivalent to half the free-space wavelength, resulting in a minimum RF phase velocity of 0.5*c*. Accounting for realistic (non-zero) waveguide wall thicknesses and cutoff frequency, the minimum RF phase velocity is approximately 0.65-0.7*c*. Given that high (> ~0.35*c*) phase velocities have a negative impact on relativistic magnetron efficiency, we see that a simple unfolding of the all cavity extraction concept is not sufficient.

To address this, the CACE uses a two-stage mode conversion process, which couples the TEM mode of two open-face resonant cavities to an orthogonally directed TEM mode in a coaxial

[10] Hoff, B.W.; Greenwood, A.D.; Mardahl, P.J.; Haworth, M.D., "All Cavity-Magnetron Axial Extraction Technique," Plasma Science, IEEE Transactions on , vol.40, no.11, pp.3046,3051, Nov. 2012

transmission line, as shown in Figure 22. The high reflex angle ($\phi \approx 350°$) of the CACE couples the TE_{11} mode directly to excite the TEM mode within a distance of only a quarter the free space wavelength, substantially shorter than the several axial wavelengths required for a typical mode matched converter.

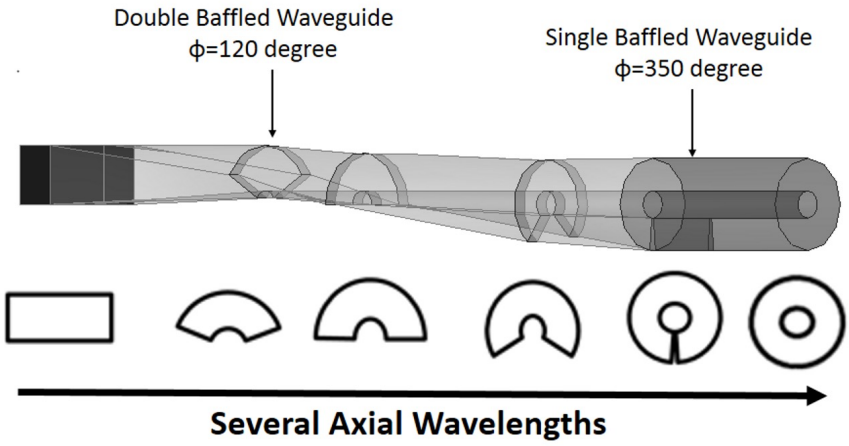

Figure 22: Converting the waveguide geometry to a coaxial geometry. An oblique 3D perspective (top) shows that this is an extension of the double baffled waveguide concept. 2D transverse cross sections (bottom) provide an additional perspective.

The initial stage of the CACE output transmission line, shown in Figure 23, is a single baffled waveguide composed of: an outer conductor (1), inner conductor (2) and baffle (3). Rectangular coupling slots (4) are used at the back-wall of adjacent cavities (5) to couple the RF electric field on either side of the anode vanes (6). Each periodic structure is repeated end to end to form a single slow-wave structure of the RPM-CACE. Top and bottom slow wave structures are separated by a distance determined by the AK gap (7) and the cathode (8) thickness. RF power coupled into the output transmission line is mono-directionally propagated in the axial direction, away from the magnetron, using a capacitively-matched shorting plate (9).

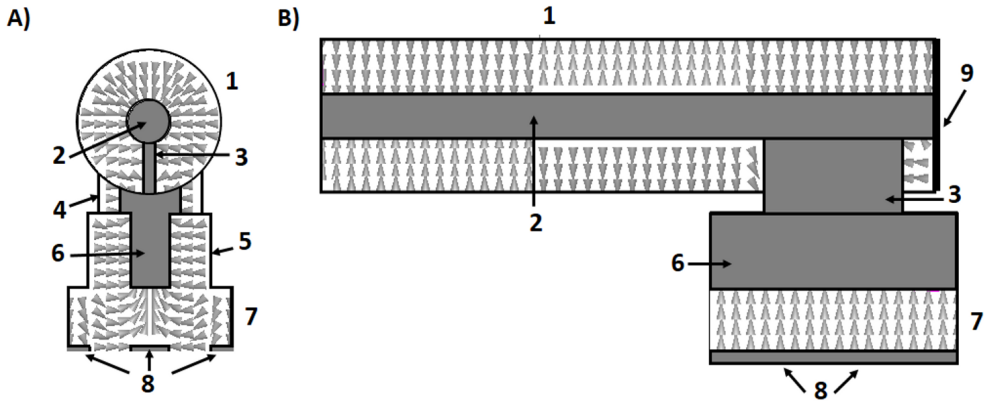

Figure 23: Electric field configurations (arrows) for the RPM CACE for the: A) Transverse cross-section, and B) Longitudinal cross-section.

To field this extraction system on the existing experimental equipment at the University of Michigan, the entire anode and extraction structure needed to fit within the 43.2 cm ID of the electromagnets. As such, the system was designed to have 12 cavities, 6 WR-340 waveguides and an operating frequency of 1.9 GHz. This kept the RF phase velocity to 0.35*c*, and operated 9% below the waveguide cutoff.

Using HFSS, ICEPIC, and the parallel computing resources available at AFRL, the dimensions shown in Figure 23 were optimized to produce operation at the target frequency, while maintaining a quality factor above the over-coupled value, determined to be ~15 by ICEPIC simulations. In simulation, the RPM-CACE was able to produce 420 MW, with a current of 2.3 kA, a voltage of 330 kV, for an efficiency of 50-70%, operating at a π-mode frequency of 1.89 GHz.

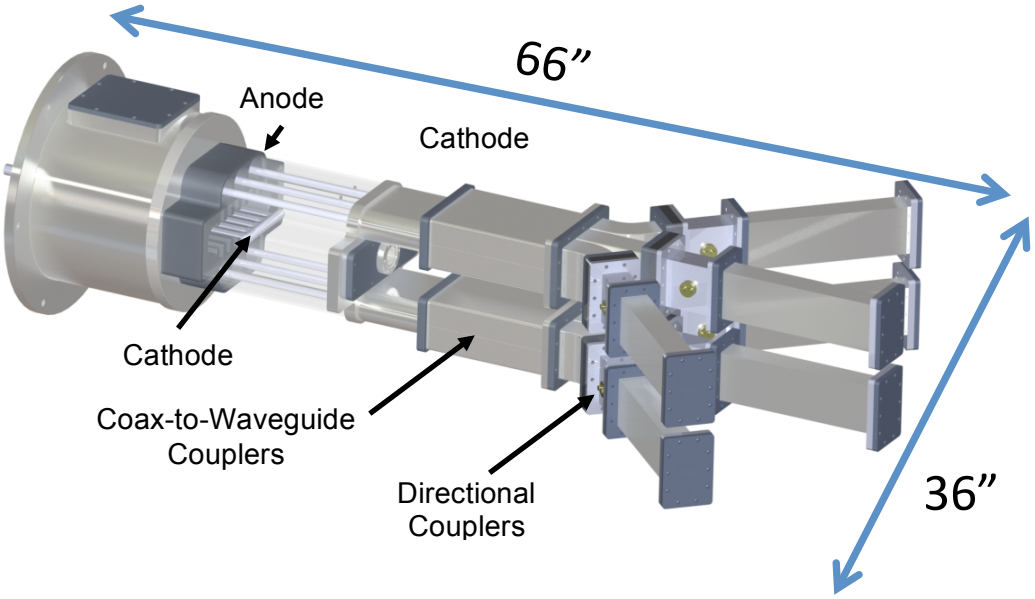

Figure 24: Solidworks model of the complete RPM-CACE. The vacuum chamber surrounding the anode and coaxial lines is removed for clarity.

This device, shown in Figure 24, has only recently completed fabrication, and is scheduled for testing in fall of 2015.

Experimental Results and Discussion

Phase Measurements

The initial tests of the RPM-12a, using the LC-1 and MCC-1 cathodes, were focused on analyzing the mode structure and spectral purity of the microwave signals generated by the RPM.

As described in the previous section, the phase measurements used a broadband load, and measured the phase of RF generated on each slow wave structure. Those signals were numerically low pass filtered (< 1.5 GHz) before frequency-locking analysis was performed. We

defined frequency-locking as a state of operation where the relative phase difference between the oscillators was static for more than 20 ns, with a +/- 10° margin of error. Using this metric, the resulting performance of each cathode designs is shown in Table 2. As this shows, each cathode demonstrated an improvement in the occurrence of frequency-locking.

Table 2: Frequency-locking percentage for various cathode designs.

Cathode	% of Locked Shots
LC-1	23
MCC-1	32
MCC-2	57

Despite generating many uniform pulses, such as the sample shown in Figure 25, the LC-1 cathode was still highly susceptible to intense mode competition (Figure 26), with only 23% of its shots demonstrating frequency-locked operation.

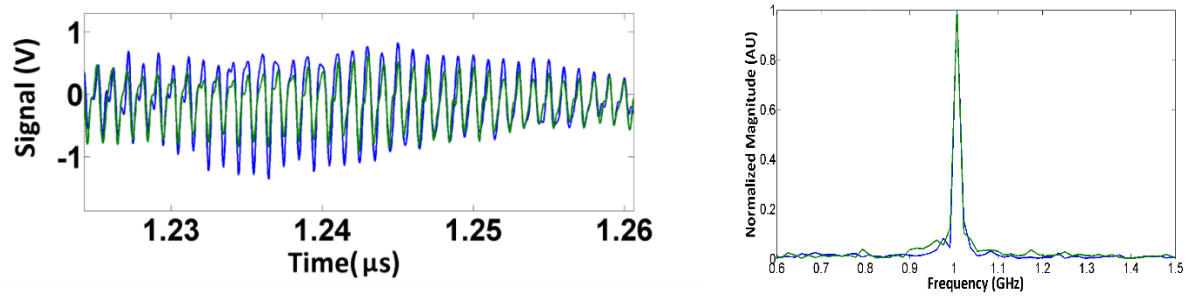

Figure 25: An example of a raw microwave signal produced by the RPM with the MCC-1 installed. Phase locking is evident (left), and the FFT (right) shows no indication of mode competition.

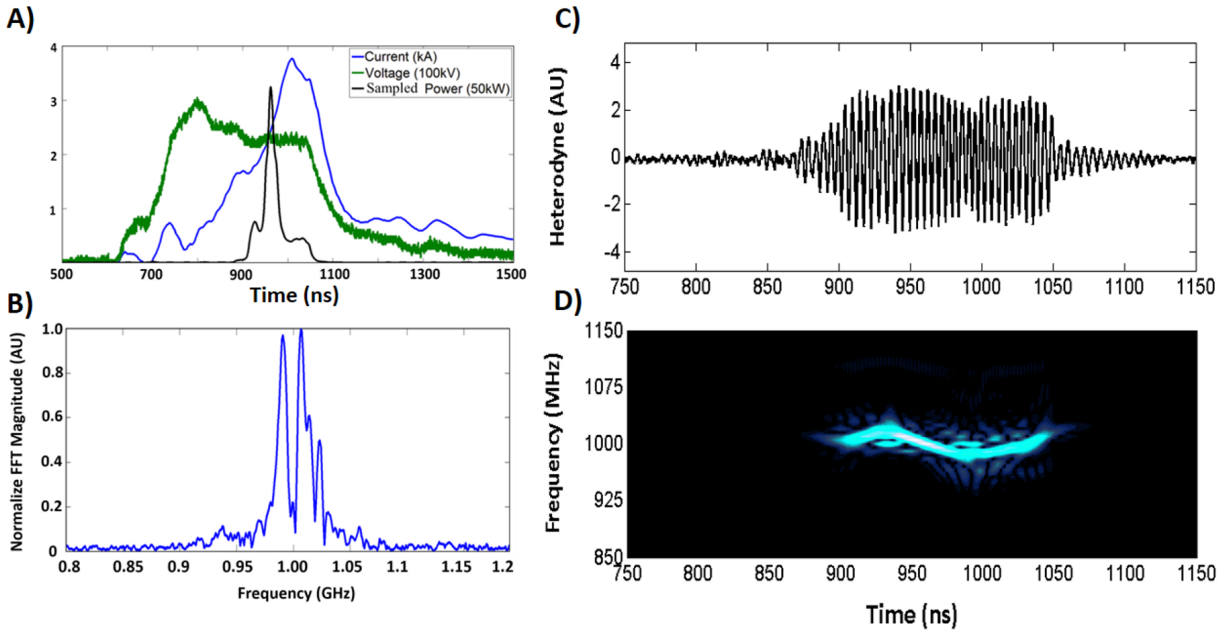

Figure 26: RPM-12a shot demonstrating strong bi-modal operation with the LC-1 cathode. A) shot profile with relevant parameters, B) raw signal from heterodyne diagnostic, C) time-integrated Fourier transform, and D) time-frequency analysis (normalized white=1 and blue=0.5 and black=0).

The MCC-1, designed specifically to improve microwave start-up and locking time, improved the percentage of frequency-locked shots to 32%, improved the average locking duration from 26 to 32 ns, and improved the average pulselength from 124 to 260 ns. The substantially improvement in pulse duration is expected to be largely due to a reduction in endloss current, courtesy of the cylindrical end caps. The MCC-1 also demonstrated faster startup and higher sampled diode power (this was an uncalibrated power measurement, but the MCC-1 had higher sampled power using the same load and power sampling setup).

The MCC-2 further improved this concept by narrowing the AK gap and improving cross-oscillator coupling, increasing the percentage of frequency-locked shots to 57%.

Power Measurements

A total of 93 shots were conducted on the RPM-12a using the configuration shown in Figure 18, allowing us to make calibrated power measurements. These shots were all conducted using the MCC-2 cathode. The initial set was with a 101 cm^2 bare aluminum emission area (Figure 10), while the second set used 36 cm^2 of velvet fabric for emission sites (Figure 11d). For these power measurements the voltage ranged from -250 to -300 kV, while the magnetic fields for the aluminum and velvet emitters were 0.23-0.27 T and 0.2-0.34 T, respectively. Typical currents at start-up for these shots ranged from 2-4 kA. An endloss current monitor was not fieldable on the power extraction setup (Figure 18), so precise endloss currents are unknown. Previous endloss measurements with the phase measurement setup (Figure 17) indicated endloss currents of less than 0.2 kA. Consequently, all quoted efficiencies are total efficiencies, rather than electronic efficiencies.

Figure 27 shows the two broad classes of shots encountered on the RPM-12a with MCC-2 cathode. Generally, the velvet emitters drew higher currents during the 100-150 ns voltage risetime. The onset of oscillations generally occurred near the peak voltage for both cathodes. After RF oscillations ceased, current continued to increase steadily due to AK gap closure, as can be seen in the figures below. Current is extinguished by a command or self-crowbar within the pulsed power driver. Damage to the anode structure occurs if the current is allowed to continue to increase as the plasma cathode expands.

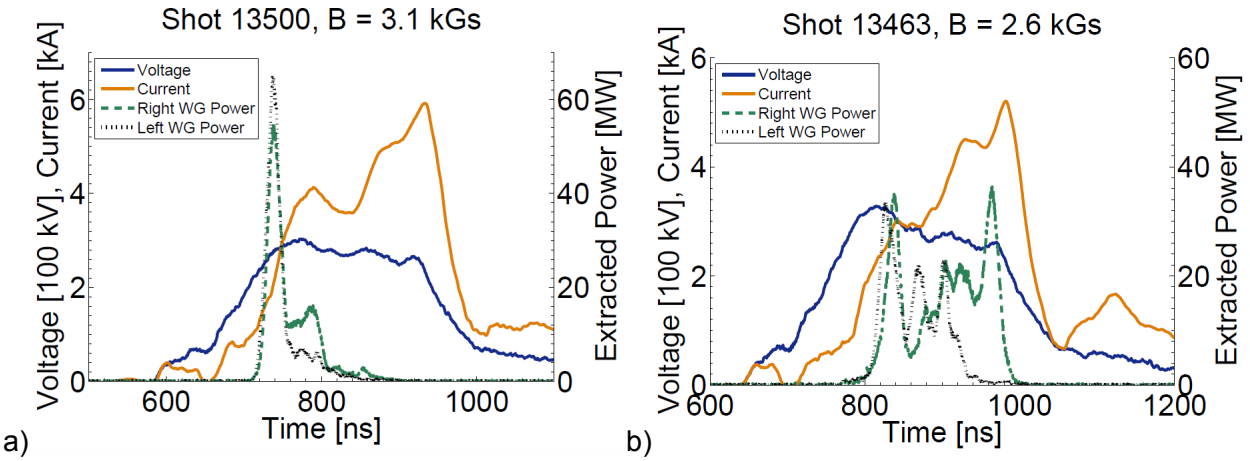

Figure 27: Sample shots illustrating the two broad types of RPM-12a operation. a) High-power (> 100 MW), short duration shot using the MCC-2 with velvet emitters. b) a moderate-power (10's MW), long-duration shot using the MCC-2 with bare aluminum emitters.

Generally, and regardless of which MCC-2 embodiment was utilized, the RPM-12a operated in either the high-power (> 100 MW), short-duration mode shown in Figure 27a, or the moderate-power (10's MW), long-duration mode of Figure 27. As the experimental configuration in the previous section indicated, we extract power from each side of the RPM independently. Consequently, the peak total power correlated strongly with a small offset between the peaks of each waveguide, as shown in Figure 28. Also notable from this figure is the fact that, while the two emitters produced similar maximum peak powers, the aluminum emitter produced a moderate (< 100 MW) peak power much more often than the velvet emitter did.

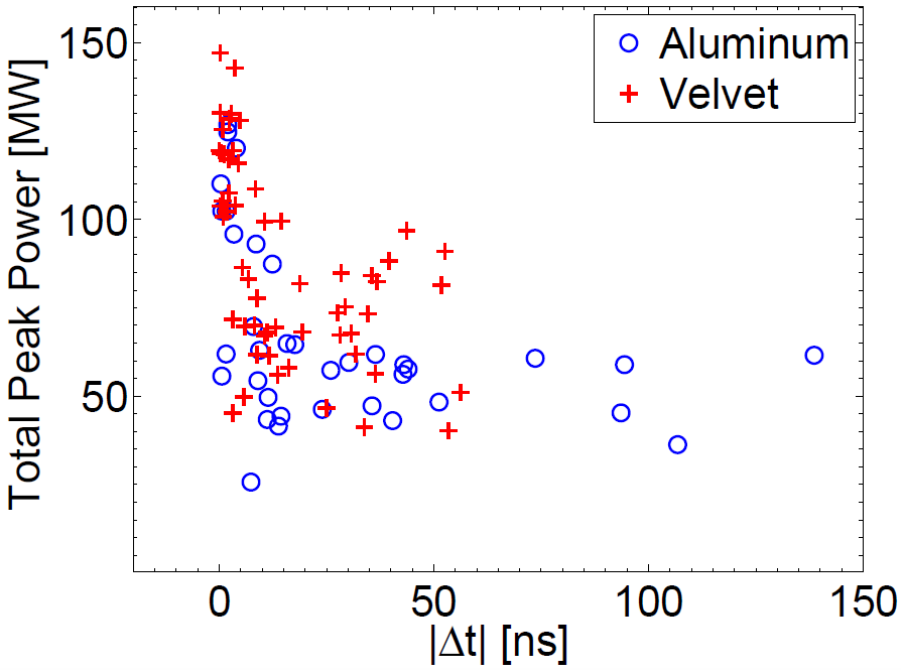

Figure 28: Peak total power as a function of the difference in time between the peak output power of each waveguide.

As Figure 29 demonstrates, we observed no correlation between output power and magnetic field. The velvet emitter was operated at much higher magnetic fields, initially due to concerns over gap closure, and later as we found it operated best at the highest field we could manage. Our electromagnets were only capable of producing a magnetic field of 0.32 T, and the output power of the velvet cathode continued to improve as we approached this value, so it is possible that we have not yet reached its optimal operating parameters.

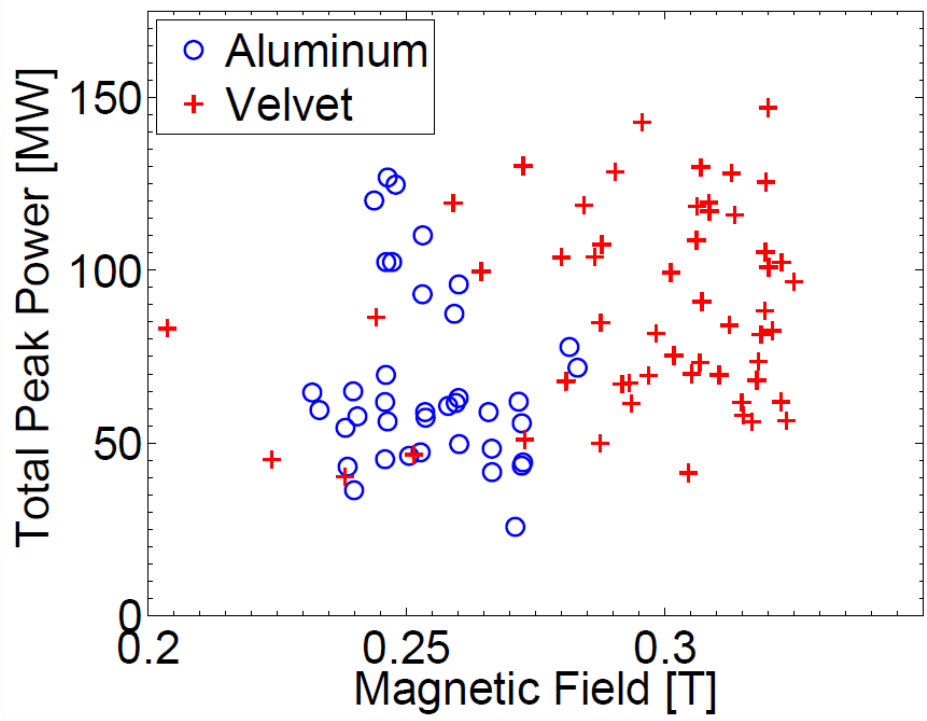

Figure 29: Peak total power vs. magnetic field for RPM-12a shots with the MCC-2 cathode.

The velvet emitter, on average, was also 50% more efficient than the bare aluminum emitter, with high power shots demonstrating peak instantaneous efficiencies of 12-32%. While some efficiency gains are expected as a result of operating at higher magnetic fields[11], simulations have also shown more uniform emission and a larger emitting area can produce increases in efficiency[12].

As shown in Table 3, the last metric we analyzed was the microwave start-up time. The reference time ($t = 0$) was defined as the time at which the voltage pulse reached half its maximum value. Again, the velvet emitter as an improvement over the bare aluminum. The lower start-up time, coupled with lower current draw during the voltage ramp, suggests that the velvet emitter began emitting at lower electric fields than the bare aluminum cathode.

[11] Y. M. Saveliev, S. Spark, B. Kerr, M. Harbour, S. Douglas, and W. Sibbett, "Effect of cathode end caps and a cathode emissive surface on relativistic magnetron operation," IEEE Trans. Plasma Sci., vol. 28, no. 3, pp. 478–484, Jun. 2000.
[12] R. Lemke, T. Genoni, and T. Spencer, "Effects that limit efficiency in relativistic magnetrons," IEEE Trans. Plasma Sci., vol. 28, no. 3, pp. 887–897, Jun. 2000.

Table 3: Performance metrics for the MCC-2 cathode types tested.

Emitter	% Shots with $\|\Delta t\| < 5$ ns	Mean Peak Efficiency [%]	Mean Time to Oscillations [ns]	Highest Peak Efficiency [%]	Highest Peak Power [MW]
Bare Al	21	10 ± 5	51 ± 21	20	129
Velvet	37	15 ± 8	23 ± 7	32	149

Conclusions

We have designed, simulated, fabricated, and characterized a novel magnetron concept, the Recirculating Planar Magnetron (RPM). Using HFSS, MAGIC and ICEPIC, we have simulated the operation of the device in both a conventional and inverted magnetron geometry, and found the conventional geometry to be more practical for extraction. After significant computational iteration, several prototypes were fabricated and tested. Initial phase measurements demonstrated mode competition between the two slow-wave structures, and poor cross-oscillator coupling through the recirculating bends. To improve coupling, and promote frequency-locked operation, the Mode Control Cathode was developed. Multiple cathode designs were simulated and tested, varying both geometry and material properties. Calibrated power diagnostics were fielded on the prototype. Ultimately, the MCC-2 cathode with velvet emitters proved to be the most effective design, demonstrating faster start-up, more consistent frequency-locking, higher mean efficiency, and more consistent high power operation than its predecessors. The RPM demonstrated peak instantaneous electronic efficiencies as high as 32%, and peak powers of up to 150 MW. A successor to the prototype, the RPM-CACE has been designed and fabricated. It has been simulated to produce 420 MW of peak power at an efficiency of 50-70%. As part of this design, a new type of coupler, the Coaxial All-Cavity Extractor, has been designed, fabricated, and tested. This coupler design allows for efficient, broad-band power extraction along the axis of a RPM with a limited diameter.

Future Work

Currently, we are adapting the RPM geometry to produce a Relativistic Planar Amplifier for the Air Force Office of Scientific Research. In the near future, the RPM-CACE will be tested and validated. In simulation, it was capable of producing RF pulses of 420 MW, a substantial power increase over what the prototype was able to demonstrate. We expect to field improve cathode materials, such as CsI-coated carbon fibers from ESLI, on all cathode designs. The use of these fibers should provide more uniform emission, faster start-up, and less plasma production, when compared to existing velvet emitters. Pending the award of a DURIP and acquisition of an Ultra-Fast Intensified Framing Camera, we aim to analyze the mode structure of the RPM via time and spatially resolved spectroscopy of RF Stark broadening. Attempts to identify the mode structure of the RPM have thus far been inconclusive. The RPM-12a will also be used as a test bed for 3D-printed HPM components, as we will be replacing its anode blocks with a metallized plastic. We are also increasing the capabilities of our electromagnets to explore the performance of the RPM above 0.32 T.

Patents

R.M. Gilgenbach, Y.Y. Lau, D. M. French, B. W. Hoff, J. Luginsland, and M.A. Franzi, “Crossed field device," US Patent No.: US8,841,867 B2, Granted September 23, 2014

Publications

Refereed Archival Journals

1) M. Franzi, G.B. Greening, N.M. Jordan, R.M. Gilgenbach, D.H. Simon, Y.Y. Lau, B.W. Hoff, J.W. Luginsland, “Microwave Power and Phase Measurements on a Recirculating Planar Magnetron”, IEEE Transactions on Plasma Science, v43, p1675 (2015)

2) Matthew Franzi, Ronald Gilgenbach, Y. Y. Lau, Brad Hoff, Geoff Greening et al., “Passive mode control in the recirculating planar magnetron” Phys. Plasmas 20, 033108 (2013); doi: 10.1063/1.4794967

3) M.A. Franzi, R.M. Gilgenbach, B.W. Hoff, D.A. Chalenski, D. Simon, Y.Y. Lau, and J.W. Luginsland, “Recirculating Planar Magnetron Simulations and Experiments”, IEEE Trans. Plasma Science V41, 639 (2013)

4) D. H. Simon, Y. Y. Lau, J. W. Luginsland, and R. M. Gilgenbach, “An unnoticed property of the cylindrical relativistic Brillouin flow,” Phys. Plasmas **19**, 043103 (2012).

5) P. Zhang, Y.Y. Lau and R.M. Gilgenbach, “Thin Film Contact resistance with –Dissimilar Materials”, J. Appl. Phys. V109, p124910 (2011)

6) Ronald M. Gilgenbach, Yue-Ying Lau, David M. French, Brad W. Hoff, Matthew Franzi and John Luginsland, “Recirculating-Planar-Magnetrons for High Power, High-Frequency Radiation Generation”, IEEE Trans. Plasma Science, V39, p980-987 (2011)

7) D.M. French, B.W. Hoff, Y.Y. Lau and R.M. Gilgenbach, “Negative, Positive and Infinite Mass Properties of a Rotating Electron Beam”, Applied Physics Letters, V97 p (2010)

Ph.D. Dissertations

“Investigation of Novel Configurations for High Power Microwave Generation” D.M. French, Ph.D. Thesis, University of Michigan, Ann Arbor, 2011.

“Relativistic Recirculating Planar Magnetrons” M.A. Franzi, Ph.D. Thesis, University of Michigan, Ann Arbor, 2014.

AFRL Reports

“A Compact, Pi-Mode Extraction Scheme for the Axial B-Field Recirculating Planar Magnetron”, Hoff, Brad W ; Franzi, M ; French, D M ; Greening, G ; Gilgenbach, R M, AFRL Technical rept. Aug 2011-Jul 2012.

Conference Papers

Gilgenbach, R.M.; Yue-Ying Lau; French, D.M.; Hoff, B.W.; Franzi, M.; Simon, D.; Luginsland, J.W., "21.1: Recirculating-planar-magnetrons for high power, high-frequency radiation generation," *Vacuum Electronics Conference (IVEC), 2010 IEEE International* , vol., no., pp.507,508, 18-20 May 2010
doi: 10.1109/IVELEC.2010.5503480

"Recirculating Planar Magnetron Modeling and Experiments" R.M. Gilgenbach, M.A. Franzi , D. M. French, B. W. Hoff, and Y.Y. Lau, 52nd APS DPP, Nov. 11, 2010.

Gilgenbach, R.M.; Lau, Y.; French, D.M.; Hoff, B.W.; Franzi, M.; Simon, D.; Luginsland, J.W., "Recirculating planar magnetrons for HPM and millimeter-wave generation," *Plasma Science, 2010 Abstracts IEEE International Conference on* , vol., no., pp.1,1, 20-24 June 2010
doi: 10.1109/PLASMA.2010.5534065

French, D.M.; Simon, D.H.; Lau, Y.Y.; Gilgenbach, R.M.; Hoff, B.W.; Luginsland, J.W., "21.2: Electron dynamics and fast startup in inverted magnetrons," *Vacuum Electronics Conference (IVEC), 2010 IEEE International* , vol., no., pp.509,510, 18-20 May 2010
doi: 10.1109/IVELEC.2010.5503481

French, D.M.; Simon, D.H.; Lau, Y.Y.; Gilgenbach, R.M.; Hoff, B.; Luginsland, J.W., "Electron dynamics and startup in crossed field microwave devices," *Plasma Science, 2010 Abstracts IEEE International Conference on* , vol., no., pp.1,1, 20-24 June 2010
doi: 10.1109/PLASMA.2010.5534066

Simon, D.H.; Lau, Y.Y.; Gilgenbach, R.M.; Tang, W.; Hoff, B.; Cartwright, K.L.; Luginsland, J.W., "Buneman-Hartree condition re-visited," *Plasma Science, 2010 Abstracts IEEE International Conference on* , vol., no., pp.1,1, 20-24 June 2010
doi: 10.1109/PLASMA.2010.5533892

Simon, D.H.; Lau, Y.Y.; Franzi, M.; French, D.M.; Gilgenbach, R.M.; Tang, W.; Hoff, B.; Cartwright, K.L.; Luginsland, J.W., "Some unusual properties of the cylindrical Brillouin flow," *Plasma Science (ICOPS), 2011 Abstracts IEEE International Conference on* , vol., no., pp.1,1, 26-30 June 2011
doi: 10.1109/PLASMA.2011.5993336

Franzi, M.; Gilgenbach, R.M.; French, D.M.; Hoff, B.W.; Lau, Y.Y.; Simon, D.; Luginsland, J.W., "Recirculating Planar Magnetron modeling and experiments," *Plasma Science (ICOPS), 2011 Abstracts IEEE International Conference on* , vol., no., pp.1,1, 26-30 June 2011
doi: 10.1109/PLASMA.2011.5993338

"Equibrium and Stability of the Brillouin Flow in Recirculating Planar Magnetron" D. H. Simon, Y. Y. Lau, M. Franzi, Geoffrey Greening, R.M. Gilgenbach, J. W. Luginsland, 54th APS-DPP, Oct 30, 2012.

Hoff, B.W.; Franzi, M.; French, D.M.; Greening, G.; Gilgenbach, R.M., "A Pi-mode extraction scheme for the axial B-field recirculating planar magnetron," *Vacuum Electronics Conference*

(IVEC), 2012 IEEE Thirteenth International , vol., no., pp.493,494, 24-26 April 2012
doi: 10.1109/IVEC.2012.6262245

"Mode Control Cathode Modeling and Experiments on a Recirculating Planar Magnetron", M. Franzi, R.M. Gilgenbach, B.W. Hoff, G.B. Greening, Y.Y. Lau, D.A. Chalenski, D.H. Simon, P. Zhang, 54th APS-DPP, Nov 2, 2012.

"Passive mode control in the recirculating planar magnetron" Franzi, Matthew and Gilgenbach, Ronald and Lau, Y. Y. and Hoff, Brad and Greening, Geoff and Zhang, Peng, Physics of Plasmas (1994-present), 20, 033108 (2013), DOI:http://dx.doi.org/10.1063/1.4794967

Franzi, M.; Gilgenbach, R.; Hoff, B.; Lau, Y.Y.; Simon, D.; French, D.; Jordan, N.M.; Luginsland, J.W., "Microwave oscillations in the Recirculating Planar Magnetron," *Vacuum Electronics Conference (IVEC), 2013 IEEE 14th International* , vol., no., pp.1,2, 21-23 May 2013. Awarded Best Student Paper.

Franzi, M.; Gilgenbach, R.M.; Hoff, B.W.; Lau, Y.Y.; Greening, G.; Chalenski, D.; Jordan, N.M.; Simon, D.; Luginsland, J.W., "Microwave oscillation, mode control and extraction in the recirculating planar magnetron," *Plasma Science (ICOPS), 2013 Abstracts IEEE International Conference on* , vol., no., pp.1,1, 16-21 June 2013
doi: 10.1109/PLASMA.2013.6633278

"Mode Control and Extraction in the Recirculating Planar Magnetron," Franzi, M.; Gilgenbach, R.M.; Hoff, B.W.; Greening, G.; Simon, D; Jordan, N.M.; Lau, Y.Y., 55th APS-DPP, Nov. 15, 2013.

Greening, Geoffrey; Franzi, Matthew; Gilgenbach, Ronald; Lau, Y.Y.; Jordan, Nicholas, "Multi-Frequency Recirculating Planar Magnetrons," *Vacuum Electronics Conference, IEEE International* , vol., no., pp.231,232, 22-24 April 2014
doi: 10.1109/IVEC.2014.6857575

Simon, D.H.; Lau, Y.Y.; Franzi, M.; Greening, G.; Gilgenbach, R.M., "Brillouin flow in recirculating planar magnetron," *Vacuum Electronics Conference, IEEE International* , vol., no., pp.383,384, 22-24 April 2014
doi: 10.1109/IVEC.2014.6857650

"Microwave Power Measurements on the Recirculating Planar Magnetron", N.M. Jordan, M.A. Franzi , G.B. Greening, R.M. Gilgenbach, D.H. Simon, Y.Y. Lau, B. W. Hoff, and J.W. Luginsland, 56th APS-DPP, Oct 31, 2014.

Franzi, M.; Gilgenbach, R.M.; Greening, G.; Jordan, N.M.; Hoff, B.W.; Simon, D.; Lau, Y.Y.; Luginsland, J.W., "Microwave extraction in the recirculating planar magnetron," *Plasma Sciences (ICOPS) held with 2014 IEEE International Conference on High-Power Particle Beams (BEAMS), 2014 IEEE 41st International Conference on* , vol., no., pp.1,1, 25-29 May 2014
doi: 10.1109/PLASMA.2014.7012355

Researchers Supported

Research Scientists supported on this grant: N.M. Jordan, P. Zhang and D. Chalenski

Students supported on this grant:

Graduate Students: M.A. Franzi, G.B. Greening, D.H. Simon, S. Patel, M. Johnson, I. Rittersdorf, H. Wood, P. Zhang and S. Exelby,

Undergraduate Students: Derek Hung, S. Richards, and R. Steinbock,

Appendix

R.M. Gilgenbach, Y.Y. Lau, D. M. French, B. W. Hoff, J. Luginsland, and M.A. Franzi, “Crossed field device," US Patent No.: US8,841,867 B2, Granted September 23, 2014, first page only

(12) **United States Patent**
Gilgenbach et al.

(10) **Patent No.: US 8,841,867 B2**
(45) **Date of Patent: Sep. 23, 2014**

(54) **CROSSED FIELD DEVICE**

(75) Inventors: **Ronald M. Gilgenbach**, Ann Arbor, MI (US); **Yue-Ying Lau**, Potomac, MD (US); **David M. French**, Ann Arbor, MI (US); **Brad W. Hoff**, Alburquerque, NM (US); **John Luginsland**, Ithaca, NY (US); **Matthew Franzi**, Chazy, NY (US)

(73) Assignee: **The Regents of The University of Michigan**, Ann Arbor, MI (US)

(*) Notice: Subject to any disclaimer, the term of this patent is extended or adjusted under 35 U.S.C. 154(b) by 473 days.

(21) Appl. No.: **12/860,336**

(22) Filed: **Aug. 20, 2010**

(65) **Prior Publication Data**

US 2011/0204785 A1 Aug. 25, 2011

Related U.S. Application Data

(60) Provisional application No. 61/235,812, filed on Aug. 21, 2009.

(51) **Int. Cl.**
H05H 7/00 (2006.01)
H01J 23/02 (2006.01)
H01J 25/42 (2006.01)

(52) **U.S. Cl.**
CPC ***H01J 25/42*** (2013.01); ***H01J 23/02*** (2013.01)
USPC **315/501**; 315/507

(58) **Field of Classification Search**
CPC H05H 7/04; H05H 13/04; H05H 7/22; H05H 9/00; H05H 13/005; H05H 7/02; H05H 13/00; H05H 13/02; H05H 7/18; H05H 9/04; H05H 11/00; H05H 1/18; H05H 2007/002; H05H 2007/025
USPC 315/501, 507, 236, 85, 267, 326, 334, 315/338, 343, 344, 348
See application file for complete search history.

(56) **References Cited**

U.S. PATENT DOCUMENTS

3,305,751	A	2/1967	Brown	
4,413,208	A *	11/1983	Morizot	315/39.3
7,265,360	B2 *	9/2007	Baker et al.	250/393
2005/0151461	A1	7/2005	Tuck et al.	
2005/0225228	A1	10/2005	Burden et al.	
2009/0108729	A1	4/2009	Gorog et al.	

OTHER PUBLICATIONS

International Search Report for PCT/US2010/046160, dated Mar. 29, 2011, 3 pages.

(Continued)

Primary Examiner — Douglas W Owens
Assistant Examiner — Jianzi Chen
(74) *Attorney, Agent, or Firm* — Reising Ethington P.C.

(57) **ABSTRACT**

A crossed field device, such as a magnetron or crossed field amplifier, that includes a cathode, an anode, one or more magnetic elements, and one or more extraction elements. In one embodiment, the crossed field device includes an annular cathode and anode that are axially spaced from one another such that the device produces an axial electric (E) field and a radial magnetic (B) field. In another embodiment, the crossed field device includes an oval-shaped cathode and anode that are radially spaced from one another such that the device produces a radial electric (E) field and an axial magnetic (B) field. The crossed field device may produce electromagnetic (EM) emissions having a frequency ranging from megahertz (MHz) to terahertz (THz), and may be used in one of a number of different applications.

34 Claims, 11 Drawing Sheets

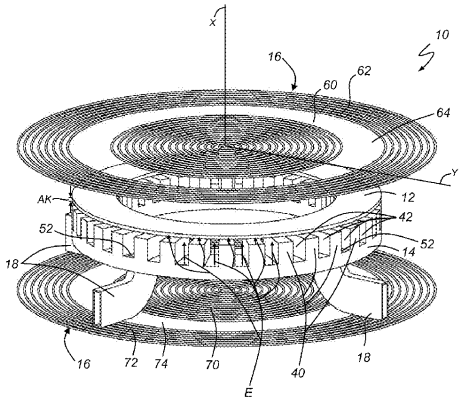

1.

1. Report Type

Final Report

Primary Contact E-mail
Contact email if there is a problem with the report.

rongilg@umich.edu

Primary Contact Phone Number
Contact phone number if there is a problem with the report

734-763-1261

Organization / Institution name

University of Michigan

Grant/Contract Title
The full title of the funded effort.

Innovative Inverted Magnetron Experiments and Theory

Grant/Contract Number
AFOSR assigned control number. It must begin with "FA9550" or "F49620" or "FA2386".

FA9550-10-1-0104

Principal Investigator Name
The full name of the principal investigator on the grant or contract.

Ronald M. Gilgenbach

Program Manager
The AFOSR Program Manager currently assigned to the award

Jason Marshall

Reporting Period Start Date

04/01/2010

Reporting Period End Date

02/28/2015

Abstract

A novel magnetron concept has been designed, simulated, fabricated, and characterized. Research at the University of Michigan has developed the Recirculating Planar Magnetron (RPM), a new type of High Power Microwave (HPM) device. Using HFSS, MAGIC, and ICEPIC, researchers have simulated the operation of the device in both a conventional and inverted magnetron geometry, and found the conventional geometry to be more practical. After significant computational iteration, several prototypes were fabricated and tested across a wide parameter space encompassing -250 to -300 kV, 0.18-0.3 T, and pulselengths of 200-500 ns. To improve device operation, multiple cathode designs were simulated and tested, varying both geometry and material properties. The RPM demonstrated peak instantaneous electronic efficiencies as high as 32%, and peak powers of up to 150 MW at 1 GHz. A patent was filed and granted on this RPM device during this grant . A 1.89 GHz variant, the RPM-CACE, has been designed and optimized in collaboration with Air Force Research Lab via an iterative design process. Its unique coupler design, the Coaxial All-Cavity Extractor (CACE), provides an efficient, broadband method of power extraction where axial power extraction is desired. In simulation, the RPM-CACE was up to 70% efficient, producing peak microwave powers of 420 MW.

Distribution Statement

This is block 12 on the SF298 form.

Distribution A - Approved for Public Release

Explanation for Distribution Statement

If this is not approved for public release, please provide a short explanation. E.g., contains proprietary information.

SF298 Form

Please attach your SF298 form. A blank SF298 can be found here. Please do not password protect or secure the PDF The maximum file size for an SF298 is 50MB.

GilgenbachForm 298F.pdf

Upload the Report Document. File must be a PDF. Please do not password protect or secure the PDF . The maximum file size for the Report Document is 50MB.

GilgenbachAFOSR FinalReport15F.pdf

Upload a Report Document, if any. The maximum file size for the Report Document is 50MB.

Archival Publications (published) during reporting period:

1) M. Franzi, G.B. Greening, N.M. Jordan, R.M. Gilgenbach, D.H. Simon, Y.Y. Lau, B.W. Hoff, J.W. Luginsland, “Microwave Power and Phase Measurements on a Recirculating Planar Magnetron”, IEEE Transactions on Plasma Science, v43, p1675 (2015)
2) Matthew Franzi, Ronald Gilgenbach, Y. Y. Lau, Brad Hoff, Geoff Greening et al., “Passive mode control in the recirculating planar magnetron” Phys. Plasmas 20, 033108 (2013); doi: 10.1063/1.4794967
3) M.A. Franzi, R.M. Gilgenbach, B.W. Hoff, D.A. Chalenski, D. Simon, Y.Y. Lau, and J.W. Luginsland, “Recirculating Planar Magnetron Simulations and Experiments”, IEEE Trans. Plasma Science V41, 639 (2013)
4) D. H. Simon, Y. Y. Lau, J. W. Luginsland, and R. M. Gilgenbach, “An unnoticed property of the cylindrical relativistic Brillouin flow,” Phys. Plasmas 19, 043103 (2012).
5) P. Zhang, Y.Y. Lau and R.M. Gilgenbach, “Thin Film Contact resistance with –Dissimilar Materials”, J. Appl. Phys. V109, p124910 (2011)
6) Ronald M. Gilgenbach, Yue-Ying Lau, David M. French, Brad W. Hoff, Matthew Franzi and John Luginsland, “Recirculating-Planar-Magnetrons for High Power, High-Frequency Radiation Generation”, IEEE Trans. Plasma Science, V39, p980-987 (2011)
7) D.M. French, B.W. Hoff, Y.Y. Lau and R.M. Gilgenbach, “Negative, Positive and Infinite Mass Properties of a Rotating Electron Beam”, Applied Physics Letters, V97 p (2010)

Changes in research objectives (if any):

Change in AFOSR Program Manager, if any:

Changed from John Luginsland to Jason Marshall

Extensions granted or milestones slipped, if any:

AFOSR LRIR Number

LRIR Title

Reporting Period

Laboratory Task Manager

Program Officer

Research Objectives

Technical Summary

Funding Summary by Cost Category (by FY, $K)

	Starting FY	FY+1	FY+2
Salary			
Equipment/Facilities			
Supplies			
Total			

Report Document

Report Document - Text Analysis

Report Document - Text Analysis

Appendix Documents

2. Thank You

E-mail user

May 28, 2015 15:01:43 Success: Email Sent to: rongilg@umich.edu